SYNTHESIS AND THERMAL RESPONSE OF PNIPAM

PREPARE BY ATRP

SYNTHESIS AND THERMAL RESPONSE OF POLY(*N*-ISOPROPYLACRYLAMIDE) PREPARE BY ATOM TRANSFER RADICAL POLYMERIZATION

By

YAN XIA, B.Sc.

A Thesis

Submitted to the School of Graduate Studies

in Partial Fulfillment of the Requirements

for the Degree

Master of Sciences

McMaster University

MASTER OF SCIENCES (2005) McMaster University

(Chemistry) Hamilton, Ontario

TITLE: Synthesis and Thermal Response of Poly(*N*-isopropylacrylamide) Prepared by Atom Transfer Radical Polymerization

AUTHOR: Yan Xia B.Sc. (Peking University, Beijing, China)

SUPERVISOR: Professor Harald D. H. Stöver

NUMBER OF PAGES: xv; 100

Abstract

Poly(*N*-isopropylacrylamide) (PNIPAM) has attracted much attention as a thermo-responsive polymer. However, the molecular weight (MW) dependence of its phase transition temperature is still controversial. This situation is largely due to the difficulty in synthesizing narrow-disperse PNIPAM. We have addressed the challenge and developed an atom transfer radical polymerization (ATRP) method to prepare narrow-disperse PNIPAM with moderate to high conversions, using branched alcohols as solvents. Aqueous solutions of these narrow-disperse PNIPAMs showed a dramatic decrease of the phase transition temperature with increasing molecular weight, as measured by turbidimetry and differential scanning calorimetry. Four other series of narrow-disperse PNIPAM with well-controlled molecular weights and with end groups of varying hydrophobicity were also synthesized by ATRP using the corresponding initiators, which enabled us to resolve the MW and end group effects. All the four series of samples showed an inverse molecular weight (MW) dependence of their phase transition temperature. The magnitude of the MW dependence decreased when using more hydrophobic end groups. The end groups were observed to have effects on the cloud point temperature, on the shape of the cloud point curves, and on the enthalpy of the phase transition.

Acknowledgements

First of all, I would like to thank my supervisor, Professor Harald Stöver, for his valuable guidance and absolute support throughout my graduate studies at McMaster. From his intelligence, enthusiasm, and encouragement, I learned not only polymer science knowledge, but more importantly how to do research.

I would also like to thank my supervisory committee member, Professor Alex Adronov, for his constant help and support on both my research and academic endeavor.

Special and sincere appreciation goes to Nick, who has been extremely helpful for my research and my English as well, and Xiangchun (Yin), who introduced the project to me. They have been the most intelligent and generous people that I have ever met. I am also sincerely grateful to other members of the Stöver Group: Erica, Lisa, Mukarram, Wenhui, Jafar, Grace and Mohit for their friendship, which made my stay very enjoyable.

Many thanks go to:

Gina Dimopoulos-Italiano and Dr. Kirk Green for their assistance with the MALDI-TOF analysis;

Frank Gibbs for his help with DSC;

Dr. Paul Berti's group for the use of the UV-vis spectrophotometer;

Dr. Richard Epand's group for the use of HS-DSC;

Laura Harrington, Dr. Don Hughes, and Brian Sayer for NMR facility;

Carol Dada and the entire Chemistry Department Staff.

Finally, I especially thank my parents for their endless support and selfless love!

Table of Contents

Chapter 3 The End Group Effect on the Thermal Response of Narrow-Disperse Poly(*N*-isopropylacrylamide) Prepared by Atom Transfer Radical Polymerization

List of Figures

List of Tables

List of Schemes

List of Abbreviations

AIBN	2,2'-azobisisobutyronitrile
ATRP	atom transfer radical polymerization
CP	2-chloropropionamide
CRP	controlled/living radical polymerization
DLS	dynamic light scattering
DMF	dimethylformamide
DMA	*N*,*N*-dimethylacrylamide
DP	degree of polymerization
ECP	ethyl 2-chloropropionate
EtOH	ethanol
GPC	gel permeation chromatography

HS-DSC	high-sensitivity differential scanning calorimetry
***i*-PrCP**	isopropyl 2-chloropropionamide
***i*-PrOH**	2-propanol
LCST	lower critical solution temperature
MALDI–TOF	matrix-assisted laser desorption ionization-time-of-flight
MCP	methyl 2-chloropropionate
MeOH	methanol
Me_6TREN	tris[2-(dimethylamino)ethyl]amine
MW	molecular weight
NIPAM	*N*-isopropylacrylamide
NMP	nitroxide mediated radical polymerization
***n*-PrOH**	1-propanol
PDEA	poly(*N*,*N*-diethylacrylamide)
PDI	polydispersity index
PDMA	poly(*N*,*N*-dimethylacrylamide)
PhCP	phenyl 2-chloropropionamide
PNIPAM	poly(*N*-isopropylacrylamide)
QTOF	quadrupole time-of-flight
RAFT	reversible addition-fragmentation transfer polymerization
***t*-BuOH**	*tert*-butyl alcohol
THF	tetrahydrofuran

Chapter 1 Introduction

1.0 Thermally Induced Phase Transition and the Lower Critical Solution Temperature

One class of stimuli-responsive polymers are polymers that undergo reversible phase transition in response to environmental stimuli, such as pH, temperature and light. They are of great interest to actively control properties of solutions and surfaces, and for building intelligent molecular switches.

Thermoresponsive polymers are an important category of stimuli-responsive polymers. They phase-separate when the temperature of their aqueous solutions is raised above a critical temperature, known as the lower critical solution temperature (LCST), to cause a sudden onset of turbidity of the solution. This is a reversible process, and the polymer solution turns transparent when the temperature drops below the LCST. This phase transition is the result of a balance between polymer-polymer and polymer-water interactions. Below the LCST, water is a good solvent for the polymer and the polymer favorably interacts with water to form a hydrated, expanded conformation. At the θ condition, the polymer-polymer and polymer-water interactions are perfectly balanced. Above the LCST, water becomes a poor solvent, the polymer-polymer interactions dominate, and phase separation takes place.[1]

On the molecular level, many thermoresponsive polymers undergo an abrupt conformational change from a state of well-solvated random coils below the LCST to a state of tightly packed globular particles above the LCST, which is defined as coil-to-

globule transition.[2-5] Below the LCST, hydrogen bonding between the hydrophilic moieties of the polymer and water significantly lowers the free energy of dissolution. This, however, is accompanied with an entropic penalty from structuring of water molecules around the hydrophobic group, which is referred to as a water cage.[6] The hydrophobic moieties on the polymer tend to aggregate to minimize the interface with water and thus to minimize the entropy loss of the system, which is known as the hydrophobic effect.[7] At higher temperature, the hydrogen bonds weaken and thus the relative magnitude of the hydrophobic effect increases, and the unfavorable entropic penalty ($T\Delta S$) is enhanced. This leads to the transition from the coiled to the denser globular structure.

Such a phase separation was thermodynamically explained as an entropy-driven process.[8,9] Upon mixing of polymer and water, the enthalpy change is exothermic ($\Delta H < 0$) due to hydrogen-bond formation between the polar groups on the polymer and water molecules, which is the initial driving force for dissolution. The entropy change is also negative ($\Delta S < 0$) due to the hydrophobic effect discussed above. The Gibbs free energy, ΔG, is defined as $\Delta G = \Delta H - T\Delta S$. At higher temperatures, the entropy term exceeds the enthalpy term, therefore once ΔG becomes positive, mixing is not favorable anymore, resulting in phase separation. Thus the LCST or the phase transition temperature, T_t, can be calculated as $T_t = \Delta H_t/\Delta S_t$.

1.1 Thermoresponsive Polymers

This thermally induced phase transition has been found in many natural biomacromolecules such as elastin-like polypeptides and methylcellulose, and a variety of synthetic polymers and surfactants[10], which include but are not limited to

1) polymers with amide groups, such as poly(*N*-substituted acrylamides), poly(*N*-acryloyl pyrrolidine), and poly(*N*-acryloyl piperidine);

2) polymers and surfactants with ether groups, such as poly(ethylene glycol), poly(ethylene glycol)/poly(propylene glycol) copolymers, and poly(vinyl methyl ether);

3) polymers with alcohol groups, such as hydroxypropyl acrylate, and poly(vinyl alcohol) derivatives.

Alternately, a polymer with an LCST can also be created by incorporating hydrophobic moieties into water-soluble polymers. This includes polymer modification as well as copolymerization of hydrophilic and hydrophobic monomers such as *N*,*N*-dimethylacrylamide with C_1–C_4 alkyl or alkoxyethyl acrylates.[11] Among the large number of thermoresponsive polymers, poly(*N*-isopropylacrylamide) (PNIPAM) has been the most widely studied since first reported by Heskins and Guillet[12] due to its reversible and sharp phase transition, biocompatibility, and most importantly its LCST around 32 °C, which is close to the physiological temperature.

PNIPAM has been employed in numerous applications in medicine, bioengineering and nanotechnology. PNIPAM bioconjugates with protein and oligonucleotide have been made that can control ligand-protein recognition, regulate enzymatic activity,[13-18] and separate enzymes[19] and DNA[20]. PNIPAM has also been

grafted onto linear polymers, [21] nanoparticles, [22] and membranes[23] to make responsive nanodevices, and onto nanotubes[24] and surfaces[25] to control their wettability. PNIPAM can also be crosslinked to form microgels as first reported by Pelton,[26] and such PNIPAM microgels, as intelligent materials, may find wide applications in areas such as drug delivery,[27] medical diagnostics,[28] photonics,[29,30] and sensor technology.[31]

1.2 Parameters Affecting the Phase Transition Temperature

The phase transition temperature of thermoresponsive polymers can be affected by several internal and external factors including:

1.2.1 Balance of the hydrophobic and the hydrophilic moieties

The balance of the hydrophobic and the hydrophilic moieties in the polymer structure determines its LCST. For example, aqueous solutions of poly(*N*,*N*-dimethylacrylamide) (PDMA) do not show LCST behavior as the two N-substituted methyl groups are not hydrophobic enough to balance the hydrophilic amide groups. In contrast, aqueous solutions of poly(*N*-ethylacrylamide) have an LCST around 73 °C.[32] Substituting another ethyl group at the amide group gives poly(*N*,*N*-diethylacrylamide) (PDEA) with a LCST of about 30 °C.[33] The LCST of aqueous solutions of PNIPAM copolymers was found to increase or decrease by increasing the fraction of hydrophilic or hydrophobic comoners, respectively.[32, 34,35]

1.2.2 Polymer microstructure

Bergbreiter et al. found that poly(*N*-n-propylacrylamide), the structural isomer of PNIPAM, has an LCST of 25 °C, approximately 5 °C lower than PNIPAM. It was proposed that the lower LCST for this polymer may reflect a slightly reduced solvent accessible area to the polymer.[36] The same tendency was found in poly(*N*-vinylalkylamide)s: when the *N*-alkyl substituent is changed from isopropyl to *n*-propyl, the LCST shifted from 39 to 32 °C.[37] Poly(*N*-vinylisobutyramide) also showed a higher LCST than its isomer PNIPAM.[37] This implies that both the hydrophobic-hydrophilic balance and the hydration structure of the polymers play an important role in the phase transition.

1.2.3 Polymer architecture

Highly branched PNIPAMs with imidazole end groups were prepared by reversible addition-fragmentation transfer (RAFT) polymerization (Figure 1). Interestingly, these highly branched PNIPAMs have lower LCSTs than the similar linear analogous PNIPAMs with equivalent mole fractions of imidazole content.[38] This was tentatively rationalized as improved aggregation of the imidazole end groups compared to the pendant imidazole groups on the linear polymers. Further investigation of these polymers in solutions by light scattering, NMR and luminescence techniques is still ongoing.

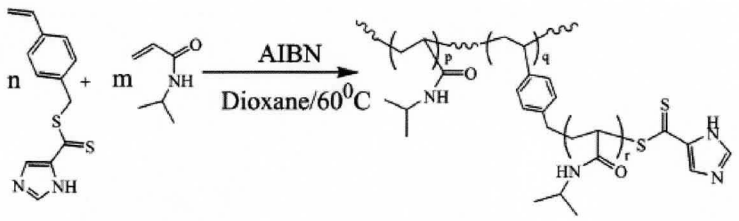

Figure 1. Highly branched PNIPAM prepared by RAFT polymerization. (from ref 38)

Poly(amidoamine) dendrimers with isobutyramide groups on the periphery were prepared and were found to have an LCST that decreases dramatically from 75 °C for generation 3 to 35 °C for generation 5.[39] It was thought that the interaction of the peripheral isobutyramide groups with each other would take place more efficiently with increasing generation of the dendrimer due to the progressive increase in the density of the terminal isobutyramide groups.

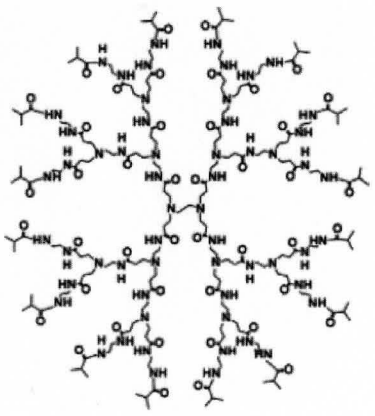

Figure 2. Isobutyramide-terminated poly(amidoamine) dendrimer (from ref 39)

1.2.4 Tacticity

The configuration of the polymer backbone can also affect its LCST. Several PDEAs were prepared by anionic, group transfer, and radical polymerization to have mainly isotactic, syndiotactic and atactic backbones, respectively. The LCSTs of PDEAs made by group transfer and by radical polymerization were 30 °C. In contrast, the LCST of the isotactic PDEA was 40 °C.[40] No simple explanation was drawn in that study as the molecular weight, polydispersity and different end groups may have also influenced the LCST.

1.2.5 Additives

In the majority of applications of thermoresponsive polymers, polymers are mixed with various cosolutes that are being delivered, removed, or are present as inert substances in the solutions. For biotechnological applications, the buffered aqueous solutions will often contain different agents to mimic physiological conditions. Therefore, much attention has been aimed at the influence of additives on the thermal phase transition of polymers, for both academic and commercial purposes. It is known that the LCST behavior will be affected by any cosolutes that can bind to the polymer or substantially change the water structure, including salts, surfactants, and cosolvents.[8]

1.2.5.1 Salt

In general, increasing salt concentration decreases the solubility of the polymer and reduces the LCST, which is called the "salting-out" effect, even though there are a

few salts, such as thiocyanate and iodide, which exhibit the opposite "salting-in" behavior. An empirical estimation of the salt effect can be obtained from the classic lyotrophic series[41]:

[Most salting-out] $SO_4^{2-} < HPO_4^{2-} < CH_3COO^- < Cl^- < Br^- < ClO_4^- < SCN^-$ [Most salting-in]

A large volume of research has been conducted to confirm this trend and understand the effect of salt on the water structure and the conformational change of polymer in phase transition.[42-47]

1.2.5.2 Surfactant

Surfactants, such as sodium dodecylsulfate (SDS), were found to bind to PNIPAM and enhance its solubility, and elevate the LCST.[44,48-50]

1.2.5.3 Cosolvent

PNIPAM is soluble in many polar organic solvents without an LCST behavior. However, Tirrell et al. and Winnik et al. have shown that adding an organic cosolvent to PNIPAM aqueous solution did not always increase the LCST.[51,52] Instead, the organic solvent/water mixture may significantly lower the LCST as a so-called "cononsolvent". For example, PNIPAM can be precipitated at room temperature from methanol/water mixture in a range of methanol/water ratios as the water-alcohol complexation reduces the interaction of polymer and water.[52]

D_2O has also been used as a solvent for PNIPAM. It was found that PNIPAM has a more extended conformation[53] and a higher LCST[36,54] in D_2O than in H_2O. The reason is not yet clear. But hydrogen bonding is approximately 5% stronger in D_2O than in H_2O, so breaking hydrogen bonds would be more enthalpically costly in D_2O.[36]

1.2.6 Pressure

In theory, pressure decreases the free volume difference between water and polymer and increases polymer solubility, so higher pressure will result in higher LCST.[55] Takahashi et al. observed an increase of the LCST of PNIPAM aqueous solution with increasing pressure up to 50 MPa, but then a decrease of the LCST with further increases of pressure.[56] Factors acting on the aggregation of polymer chains under high pressure were not clear, but the authors suggested that the uncertain molecular weights and broad polydispersities of the samples studied may have affected the precise investigation.

1.2.7 Concentration

Numerous studies using turbidimetry have shown that the LCSTs of PNIPAM and other thermoresponsive polymers decrease with increasing polymer concentration.[33,45,57-59] The dependence is usually more significant in the very dilute range. Occasional reports claimed independence of the LCST on concentration.[3a] It is worth noting that Winnik et al. also reported that the LCST is independent of the concentration, at least in a dilute range, from their studies of thermoresponsive polymer solutions by microcalorimetry.[60,61]

1.2.8 Molecular weight

The molecular weight (MW) dependence of the LCST of polymers has been a very attractive and controversial topic. The LCSTs of NIPAM homopolymers have been reported to be inversely dependent,[42] directly dependent,[57] or independent[3a,4b,62,63] of the molecular weight. A similar situation exists for other thermoresponsive polymers including other polyacrylamides.[33,58-61,64-66] While the use of different initiators and hence end groups, different polymer concentrations and different techniques for measuring LCSTs accounts for some of these variations, most of previous studies also relied on partially fractionated[3a,4b,57,62] or unfractionated[42] PNIPAM samples obtained from conventional radical polymerizations, which often had broad polydispersities. These polydisperse samples may have precluded precise examination of molecular weight effects on LCST, because the low or high molecular weight fraction, whichever has a lower LCST, may mask the LCST of the bulk of the sample, particularly as measure by turbidimetry. A definitive answer hence would require the synthesis of PNIPAMs with well-controlled molecular weights and end groups. Furthermore, the broad polydispersities of the samples used for other studies of the LCST dependence upon parameters, such as polymer microstructure, tacticity, and pressure, may have also affected their accuracy as some authors have already pointed out.

To clarify this controversial situation, we set our initial research goal to prepare narrow-disperse PNIPAMs with well-controlled molecular weights and end groups, using atom transfer radical polymerization (ATRP).

1.3 Atom Transfer Radical Polymerization (ATRP) of NIPAM

Significant progress in the field of controlled/living radical polymerization (CRP) has been achieved over the past decade, which has enabled the synthesis of various homopolymers and copolymers with predetermined molecular weight, low polydispersity, well defined composition, functionality, and chain architecture.[67-69] All the CRP methods are based on the same idea:

1) A dynamic equilibrium is established between a low concentration of active propagating chains and a large amount of dormant chains, which are unable to propagate or terminate, via rapid, reversible termination or chain transfer reaction;

2) The propagation and the deactivation of the active radicals, namely reversible termination or chain transfer reaction, are much faster than any irreversible termination to minimize the chance of irreversible termination and ensure that all polymer chains are growing at approximately the same rate to obtain uniform molecular weight distribution;

3) A fast and quantitative initiation is required to initiate all chains simultaneously.

ATRP has been one of the best developed CRP methods since its invention in 1995.[71,72] ATRP uses a catalytic amount of a transition metal complex, where copper complexed with nitrogen-based ligand is most widely used, to reversibly abstract a halogen atom from a polymer chain end, and thereby transform the chain end group into an active propagating radical from a dormant state. This dynamic equilibrium, shown in Scheme 1, strongly favors the left hand side ($K_{eq} = 10^{-9}$–10^{-7}). Therefore only a minute concentration of growing free radicals is maintained, and bimolecular termination and disproportionation are minimized.

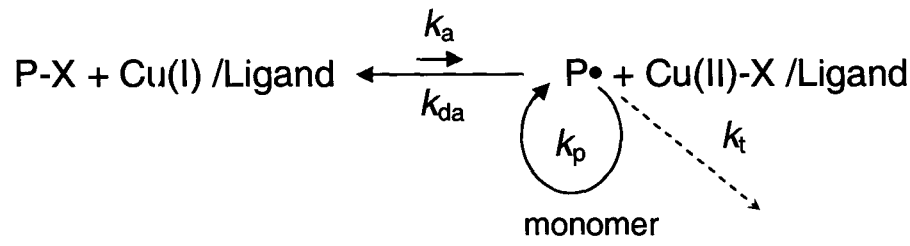

Scheme 1. Mechanism of ATRP

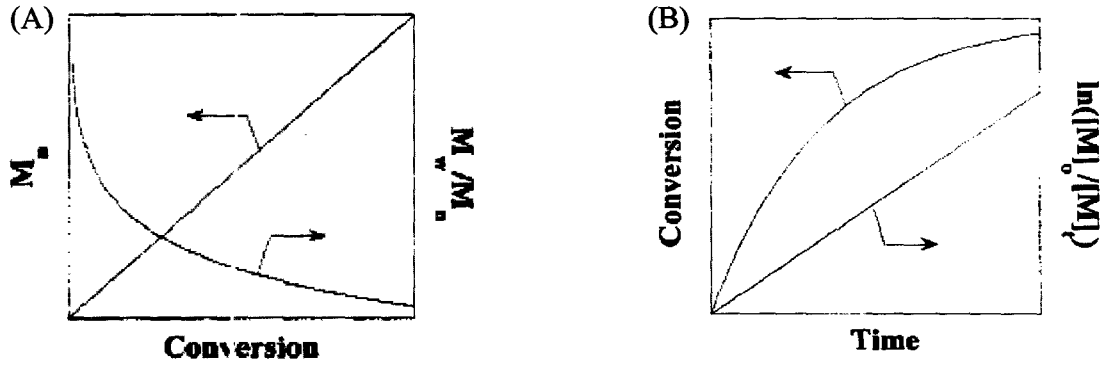

Figure 3. Schematic representation of (A) the evolution of the molecular weights and polydispersities with conversion for a living polymerization; (B) the dependence of the conversion on time in linear and semilogarithmic coordinates. (from Ref 1 (a))

In a well controlled living polymerization, the number of growing chains is constant and equal to the initial initiator concentration. The theoretical molecular weight or degree of polymerization (DP) can be predicted by the equation: $DP = [M]_0/[initiator]_0 \times$ conversion. A linear increase of the molecular weights with conversion and a progressive decrease of polydispersities as illustrated in Figure 3 (A) are typical characteristics of CRP. As shown in Figure 3 (B), a linear variation of conversion with

time in semilogarithmic coordinates is a typical kinetic characteristic of CRP, which indicates that the concentration of active species in the polymerization is constant and that the kinetics are first order with respect to monomer.

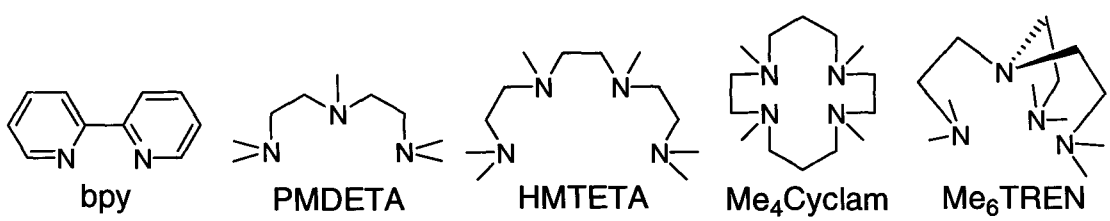

Figure 4. Structures of the ligands used in the ATRP of DMA

ATRP has been used to polymerize various monomers such as styrenes, (meth)acrylates, dienes, and acrylonitrile. However, ATRP of (meth)acrylamides has remained challenging until very recently. *N,N*-Dimethylacrylamide has been used as a model monomer to study ATRP of acrylamides. When linear amine ligands, such as *N,N,N',N',N''*-pentamethylethylenetriamine (PMDETA) and 1,1,4,7,10,10-hexamethyltriethylenetetraamine (HMTETA), and bipyridine (bpy) based ligands were used in conjunction with CuBr, the catalyst afforded only very low conversions or even failed to initiate the polymerization.[72-74] Using a very strongly activating cyclic ligand, 1,4,8,11-tetrametyl-1,4,8,11-tetraazacyclotetradecane (Me_4Cyclam), gave high conversions in relatively shorter times, however the polymerization was uncontrolled with PDI > 2.[72,74] This resulted from slow deactivation for the Me_4Cyclam system. Also, it was found that the copper catalyst can be inactivated by complexation with the polymer and monomer through the amide group and the amide group can also displace the

terminal bromine atom.[72,74] Based on these findings, alkyl chlorides rather than bromides were used as the initiators at relatively low temperatures to reduce the nucleophilic displacement of terminal C-X bond, together with a strong ligand, tris[2-(dimethylamino)ethyl]amine (Me_6TREN), which has a lower catalytic activity than Me_4Cyclam. Polymerization carried out in toluene was controlled, but it stopped at low to moderate conversions.[75] Higher conversions were obtained with higher catalyst/initiator ratio to compensate the catalyst lost during polymerization.[76] A successful ATRP of NIPAM was achieved in 1:1 (v/v) mixtures of dimethylformamide (DMF)/water at. Polymerizations were very fast with high conversions, but degrees of polymerization (DP) of 200 still required higher catalyst/initiator ratios.[77] Our group studied ATRP of DMA by exploring the effects of solvents on the polymerization and found that using a hydrogen-bonding solvent, methanol, gave high conversions and low PDI without adding excess catalyst.[78] It was believed that hydrogen-bonding between amide groups and the solvent might prevent them from deactivating the catalyst. Similar approaches have been used in the ATRP of another strongly coordinating monomer, vinylpyridine.[79]

We planned to extend this approach to ATRP of NIPAM to obtain narrow-disperse PNIPAM with controlled molecular weights and end groups.

References

(1) Finch, C. A. Ed. *Chemistry and Technology of Water-Soluble Polymers* Plenum Press: New York, 1983.

(2) Ptitsyn, O. B.; Kron, A. K.; Eizner, Y. Y. *J. Polym. Sci., Part C.* **1968,** 3509-3517.

(3) (a) Fujishige, S.; Kubota, K.; Ando, I. *J. Phys. Chem.* **1989**, *93,* 3311-3313. (b) Kubota, K.; Fujishige, S.; Ando, I. *J. Phys. Chem.* **1990**, *94*, 5154-5158.

(4) (a) Tiktopulo, E. I.; Bychkova, V. E.; Rička, J.; Ptitsyn, O. B. *Macromolecules* **1994**, *27*, 2879-2882. (b) Tiktopulo, E. I.; Uversky, V. N.; Lushchik, V. B.; Klenin, S. I.; Bychkova, V. E.; Ptitsyn, O. B. *Macromolecules* **1995**, *28*, 7519-7524.

(5) (a) Wang, X.; Qiu, X.; Wu, C. *Macromolecules* **1998**, *31*, 2972-2976. (b) Wang, X.; Wu, C. *Macromolecules* **1999**, *32*, 4299-4301.

(6) (a) Luan, C.; Harris, R. D.; Prasad, K. U.; Urry, D. W. *Biopolymer* **1990**, *29*, 1699. (b) Luan, C.; Urry, D. W. *J. Phys. Chem.* **1991**, *95*, 7896-7900.

(7) Ben-Naim, A. *Hydrophobic Interactions* Plenum Press: New York, 1980.

(8) Schild, H. G. *Prog. Polym. Sci.* **1992**, *17*, 163-249.

(9) Urry, D. W. *J. Phys. Chem. B.* **1997**, *101*, 11007-11028.

(10) Hoffman, A. S.; Stayton, P. S. *Macromol. Symp.* **2004**, *207*, 139-151.

(11) Mueller, K. F. *Polymer* **1992**, *33*, 3470-3476.

(12) Heskins, M.; Guillet, J. E. *J. Macromol. Sci. Chem.* **1968**, *A2*, 1441-1455.

(13) Stayton, P. S.; Shimoboji, T.; Long, C.; Chilkoti, A.; Chen, G.; Harris, J. M.; Hoffman, A. S. *Nature* **1995**, *378*, 472-474.

(14) Ding, Z.; Long, C. J.; Hayashi, Y.; Elmus, E. V.; Hoffman, A. S.; Stayton, P. S. *Bioconj. Chem.* **1999**, *10*, 395-400.

(15) Bulmus, V.; Ding, Z.; Long, C. J.; Stayton, P. S.; Hoffman, A. S. *Bioconj. Chem.* **2000**, *11*, 78-83.

(16) Ding, Z.; Fong, R. B.; Long, C. J.; Stayton, P. S.; Hoffman, A. S. *Nature* **2001**, *411*, 59-62.

(17) Pennadam, S. S.; Lavigne, M. D.; Dutta, C. F.; Firman, K.; Mernagh, D.; Gorecki, D. C.; Alexander, C. *J. Am. Chem. Soc.* **2004**, *126,* 13208-13209.

(18) Bontempo, D.; Maynard, H. D. *J. Am. Chem. Soc.* **2005**, *127,* 6508-6509.

(19) Chen, G. H.; Hoffman, A. S. *J. Biomed. Mater. Res.* **1998**, *39*, 498-505.

(20) Umeno, D.; Mori, T.; Maeda, M. *Chem. Commun.* **1998**, 1433-1434.

(21) Li, C.; Gunari, N.; Fischer, K.; Janshoff, A.; Schmidt, M. *Angew. Chem. Int. Ed.* **2004**, *43,* 1101-1104.

(22) Zhu, M.; Wang, L.; Exarhos, G. J.; Li, A. D. Q. *J. Am. Chem. Soc.* **2002**, *126,* 2656-2657.

(23) Ito, T.; Hioki, T.; Yamaguchi, T.; Shinbo, T.; Nakao, S.; Kimura, S. *J. Am. Chem. Soc.* **2002**, *124,* 7840-7846.

(24) Sun, T.; Liu, H.; Song, W.; Wang, X.; Jiang, L.; Li, L.; Zhu, D. *Angew. Chem. Int. Ed.* **2004**, *43,* 4663-4666.

(25) Sun, T.; Wang, G.; Feng, L.; Liu, B.; Ma, Y.; Jiang, L.; Zhu, D. *Angew. Chem. Int. Ed.* **2004**, *43,* 357-360.

(26) Pelton, R. *Adv. Colloid Interface Sci.* **2000**, *85*, 1-33.

(27) Nolan, C. M.; Serpe, M. J.; Lyon, L. A. *Biomacromolecules* **2004**, *5*, 1940-1946.

(28) Nayak, S.; Lee, H.; Chmielewski, J.; Lyon, L. A. *J. Am. Chem. Soc.* **2004**, *126,* 10258-10259.

(29) Weissman, J. M.; Sunkara, H. B.; Tse, A. S.; Asher, S. A. *Science* **1996**, *274*, 959-960.

(30) Jones, C. D.; Serpe, M. J.; Schroeder, L.; Lyon, L. A. *J. Am. Chem. Soc.* **2003**, *125*, 5292-5293.

(31) Hu, Z.; Chen, Y.; Wang, C.; Zheng, Y.; Li, Y. *Nature* **1998**, *393*, 149-152.

(32) Taylor, L. D.; Cerankowski, L. D. *J. Polym. Sci. Polym. Chem. Ed.* **1975**, *13*, 2551.

(33) Lessard, D. G.; Ousalem, M.; Zhu, X. X. *Can. J. Chem.* **2001**, *79*, 1870-1874.

(34) Feil, H.; Bae, Y. H.; Feijen, J. *Macromolecules* **1993**, *26*, 2496-2500.

(35) Barrer, L. C.; Cowie, J. M. G.; Huckerby, T. N.; Shaw, D. A.; Soltar, I.; Swanson, L. *Macromolecules* **2003**, *36*, 7765-7770.

(36) Mao, H.; Li, C.; Zhang, Y.; Furyk, S.; Cremer, P. S.; Bergbreiter, D. E. *Macromolecules* **2004**, *37*, 1031-1036.

(37) Suwa, K.; Morishita, K.; Kishida, A.; Akashi, M. *J. Polym. Sci. A: Polym. Chem.* **1997**, *35*, 3087-3094.

(38) Carter, S.; Hunt, B.; Rimmer, S. *Macromolecules* **2005**, *38*, 4595-4603.

(39) Haba, Y.; Harada, A.; Takagishi, T.; Kono, K. *J. Am. Chem. Soc.* **2004**, *126*, 12760-12761.

(40) Freitag, R.; Baltes, T.; Eggert, M. *J. Polym. Sci. A: Polym. Chem.* **1994**, *32*, 3019-3030.

(41) von Hippel, P. H.; Wong, K. *Science* **1964**, *145*, 577-580.

(42) Schild, H. G.; Tirrell, D. A. *J. Phys. Chem.* **1990**, *94*, 4352-4356.

(43) Park, T. G.; Hoffman, A. S. *Macromolecules* **1993**, *26*, 5045-5048.

(44) Baltes, T.; Garret-Flaudy, F.; Freitag, R. *J. Polym. Sci. A: Polym. Chem.* **1999**, *37*, 2977-2989.

(45) Maeda, Y.; Nakamura, T.; Ikeda, I *Macromolecules* **2002**, *35*, 217-222.

(46) Freitag, R.; Garret-Flaudy, F *Langmuir* **2002**, *18*, 3434-3440.

(47) Krasovitski, E.; Cohen, Y.; Bianco-Peled, H. *J. Polym. Sci. B: Polym. Phys.* **2004**, *42*, 3713-3720.

(48) Schild, H. G.; Tirrell, D. A. *Langmuir* **1991**, *7*, 665-671.

(49) Cabane, B.; Lee, L. T. *Macromolecules* **1997**, *30*, 6559-6566.

(50) Garret-Flaudy, F.; Freitag, R. *J. Polym. Sci. A: Polym. Chem.* **2000**, *38*, 4218-4229.

(51) Schild, H. G.; Muthukumar, M.; Tirrell, D. A. *Macromolecules* **1991**, *24*, 948-952.

(52) Winnik, F.; Ringsdorf, H.; Venzmer, J. *Macromolecules* **1991**, *23*, 2415-2416.

(53) Wang, X.; Wu, C. *Macromolecules* **1991**, *32*, 4299-4301.

(54) Kujawa, P.; Winnik, F. *Macromolecules* **2001**, *34*, 4130-4135.

(55) Patterson, D. *Macromolecules* **1969**, *2*, 672-677.

(56) Otake, K.; Karaki, R.; Ebina, T.; Yokoyama, C.; Takahashi, S. *Macromolecules* **1993**, *26*, 2194-2197.

(57) Tong, Z.; Zeng, F.; Zheng, X.; Sato, T. *Macromolecules* **1999**, *32*, 4488-4490.

(58) Kunugi, S.; Tada, T.; Tanaka, N.; Yamamoto, K.; Akashi, M. *Polym. J.* **2002**, *34*, 383-388.

(59) Xue, W.; Huglin, M.B.; Jones, T.G.J. *Macromol. Chem. Phys.* **2003**, *204*, 1956-1965.

(60) Laukkanen, A.; Valtola, L.; Winnik, F. M.; Tenhu, H. *Macromolecules* **2004**, *37*, 2268-2274.

(61) Diab, C.; Akiyama, Y.; Kataoka, K.; Winnik, F. M. *Macromolecules* **2004**, *37*, 2556-2562.

(62) Otake, K.; Inomata, H.; Konno, M.; Saito, S. *Macromolecules* **1990**, *23*, 283-289.

(63) Okada, Y.; Tanaka, F. *Macromolecules* **2005**, *38*, 4465-4471.

(64) Aoshima, S.; Oda, H.; Kobayashi, E *J. Polym. Sci. A: Polym. Chem.* **1992**, *30*, 2407-2413.

(65) Bütün, V.; Armes, S. P.; Billingham, N. C. *Polymer* **2001**, *42*, 5993-6008.

(66) Liu, Q.; Yu, Z.; Ni, P. *Colloid Polym. Sci.* **2004**, *282*, 387-393.

(67) (a) Matyjaszewski, K.; Xia, J. *Chem. Rev.* **2001**, *101*, 2921-2990. (b) Kamigaito, M.; Ando, T.; Sawamoto, M. *Chem. Rev.* **2001**, *101*, 3689-3746.

(68) Hawker, C. J.; Bosman, A. W.; Harth, E. *Chem. Rev.* **2001**, *101*, 3661-3688.

(69) Chiefari, J.; Chong, Y. K.; Ercole, F.; Kristina, J.; Jeffery, J.; Le, T. P. T.; Mayadunne, R. T. A.; Meijs, G. F.; Moad, C. L.; Moad, G.; Rizzardo, E.; Thang, S. H. *Macromolecules* **1998**, *31*, 5559-5562.

(70) Wang, J.-S.; Matyjaszewski, K. *Macromolecules* **1995**, *28*, 7901-7910.

(71) Wang, J.-S.; Matyjaszewski, K. *J. Am. Chem. Soc.* **1995**, *117*, 5614-5615.

(72) Teodorescu, M.; Matyjaszewski, K. *Macromolecules* **1999**, *32*, 4826-4831.

(73) Li, D.; Brittain, W. J. *Macromolecules* **1998**, *31*, 3852-3855.

(74) Rademacher, J. T.; Baum, M.; Pallack, M. E.; Brittain, W. J.; Simonsick, W. J. *Macromolecules* **2000**, *33*, 284-288.

(75) Teodorescu, M.; Matyjaszewski, K. *Macromol. Rapid Commun.* **2000**, *21*, 190-194.

(76) Neugebauer, D.; Matyjaszewski, K. *Macromolecules* **2003,** *36*, 2598-2603.

(77) Masci, G.; Giacomelli, L.; Crescenzi, V. *Macromol. Rapid Commun.* **2004**, *25*, 559-564.

(78) Yin, X.; Stöver, H. D. H. *Macromolecules*, **2005**, *38*, 2109-2115.

(79) Xia, J.; Zhang, X.; Matyjaszewski, K. *Macromolecules* **1999**, *32*, 3531-3533.

Chapter 2 The Thermal Response of Narrow-Disperse Poly(*N*-isopropylacrylamide) Prepared by Atom Transfer Radical Polymerization

Abstract

Room temperature atom transfer radical polymerizations of *N*-isopropylacrylamide (NIPAM) carried out in 2-propanol (*i*-PrOH) and *tert*-butyl alcohol (*t*-BuOH) resulted in PNIPAMs with polydispersities between 1.1 and 1.2, and degrees of polymerization of up to 300. Methyl 2-chloropropionate (MCP), copper(I) chloride and tris[2-(dimethylamino)ethyl]amine (Me_6TREN) were used as initiator, catalyst, and ligand in a 1:1:1 ratio. Conversions were as high as 91 and 79%, respectively, without the need for excess catalyst as was required in previous studies. Aqueous solutions of these narrow-disperse PNIPAMs showed a strong decrease of the phase transition temperature with increasing molecular weight, as measured by turbidimetry and differential scanning calorimetry. In low molecular weight samples, containing significant oligomeric fractions, the slightly hydrophobic methyl propionate end group becomes significant and further decreases the onset temperature of the phase transition. This chapter has been reproduced with permission from *Macromolecules* **2005**, *38*, 5937-5943. Copyright 2005 American Chemical Society.

2.0 Introduction

Polymers such as poly(*N*-isopropylacrylamide) (PNIPAM) and its copolymers that can respond to external stimuli are of great interest for the design of "intelligent" materials.[1-4] Aqueous solutions of PNIPAM exhibit a reversible liquid-solid phase transition with a lower critical solution temperature (LCST) around 32 °C. This LCST phenomenon is attributed to the entropy increase from the loss of hydrophobic interactions between the isopropyl groups of the polymer and water upon heating.[1, 2, 5-7]

While there have been extensive studies regarding the effects of polymer concentration,[1,8] cosolvent,[9, 10] pressure[11] and the presence of salts[7] or surfactants,[12, 13] the effect of molecular weight on the LCST of PNIPAM is not yet clear. As discussed in Chapter 1, the LCSTs of NIPAM homopolymers have been reported to be inversely dependent,[6] directly dependent,[8] or independent[5,14,15] of the molecular weight. Studies on other thermoresponsive polymers including other polyacrylamides have also shown a large discrepancy in the influence of molecular weight.[16-22] This situation is mainly due to the lack of narrow-disperse polymer samples. The polydisperse samples used for previous studies may have precluded precise examination of molecular weight effect on LCST. A definitive answer hence would require the synthesis of PNIPAMs with well-controlled molecular weights and end groups.

The preparation of linear narrow-disperse PNIPAM by reversible addition-fragmentation transfer (RAFT) polymerization[23] was recently reported[24-27] and nitroxide mediated radical polymerization (NMP)[28] was used to graft PNIPAM from a polystyrene star macroinitiator.[29] Atom transfer radical polymerization (ATRP)[30] is especially

attractive as it can provide good control over both polymer molecular weight and end groups, however the ATRP of acrylamides including NIPAM has remained challenging. The groups of Matyjaszewski and Brittain reported that ATRP of *N,N*-dimethylacrylamide (DMA) suffered from (a) deactivation of the copper catalyst through complexation with amide groups, (b) displacement of the terminal halide atom by amide groups, and (c) low values of the ATRP equilibrium constant.[31,32] Using alkyl chlorides rather than bromides as initiators in conjunction with tris[2-(dimethylamino)ethyl]amine (Me_6TREN) as ligand improved the control, though high conversions typically required high catalyst-to-initiator ratios (2:1 or 3:1).[33,34] Recently, Masci et al. reported the successful ATRP of NIPAM in dimethylformamide/water mixtures; however, degrees of polymerization (DP) of 200 still required higher catalyst/initiator ratios, likely again due to extensive catalyst deactivation.[35]

Our group recently studied linear[36-40] and cross-linked[38, 39] thermoresponsive polymers, including copolymers of DMA with hydrophobic comonomers suitable for subsequent cross-linking such as glycidyl methacrylate and allyl methacrylate.[38,39] As part of that work, we prepared DMA/*N*-phenylacrylamide copolymers with narrow molecular weight distributions using ATRP in methanol and methanol/water mixtures.[40]

In this chapter, we describe the synthesis of PNIPAM by ATRP in alcohols, using methyl 2-chloropropionate (MCP)/CuCl/Me_6TREN (1:1:1) as the initiating system (Scheme 1). We then describe for the first time the molecular weight dependence of the cloud points of aqueous solutions of narrow-disperse PNIPAM.

Scheme 1. ATRP of NIPAM

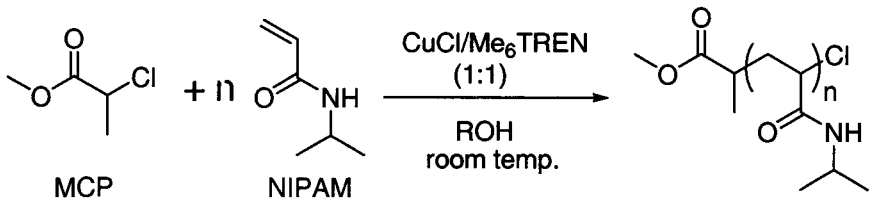

2.1 Experimental Section

2.1.1 Materials. *N*-Isopropylacrylamide (Aldrich, 97%) was recrystallized twice from benzene/hexane prior to use. Copper(I) chloride (97%), copper(II) chloride (99.99%), methyl 2-chloropropionate (97%), and tetrabutylammonium bromide (99%) were purchased from Aldrich and used as received. Me_6TREN was prepared as described in the literature.[41] Methanol (MeOH, Caledon, HPLC grade), ethanol (EtOH, Commercial Alcohols), 1-propanol (*n*-PrOH, Fisher, Certified), 2-propanol (*i*-PrOH, Fisher, HPLC grade), *tert*-butyl alcohol (*t*-BuOH, Fisher, Certified), tetrahydrofuran (THF, Caledon, HPLC grade) and pentane (Caledon, >98%) were used as received. Azobis(isobutyronitrile) was obtained as a gift from Dupont.

2.1.2 General Procedure for ATRP of NIPAM. To prepare PNIPAM with target degree of polymerization of 50, NIPAM (2.00 g, 17.7 mmol), CuCl (0.035 g, 0.35 mmol), and 2-propanol (4.00 g), deoxygenated by bubbling with nitrogen for at least 30 min, were combined and then transferred to a nitrogen-purged 25 mL round-bottom flask fitted with a septum. Me_6TREN (0.081 g, 0.35 mmol) was added via a nitrogen-purged syringe and the solution was stirred for 20 min to allow formation of the CuCl/Me_6TREN complex. MCP (0.043 g, 0.35 mmol) was then added using a syringe to begin the polymerization. The reactions were carried out at room temperature under a slight

positive pressure of nitrogen.

Aliquots (0.6 mL) were removed at regular intervals, divided between two vials in a 5:1 ratio, and dried under a stream of air. The smaller sample was dissolved in THF, passed through a short silica column to remove the catalyst, dried under a stream of air and used for gel permeation chromatography (GPC) analysis. The larger portion of the aliquot was used to determine conversion in one of two ways. For polymerizations in MeOH or *t*-BuOH, conversion was measured directly with ^{1}H NMR spectroscopy in D_2O by comparison of the peak areas of monomer signals at 5.7 ppm (one proton) or 6.2 ppm (two protons) with the polymer signal at 3.9 ppm (one proton) corrected for contribution due to monomer. For reactions in EtOH, *n*-PrOH, or *i*-PrOH, the dried sample was first reprecipitated from THF into pentane (1:12 v/v) and dried to constant weight under vacuum at 60 °C. Conversion was then determined gravimetrically and corrected for residual monomer using ^{1}H NMR spectroscopy.

2.1.3 Conventional Free Radical Polymerization of NIPAM. NIPAM (0.5 g, 4.4 mmol), AIBN (7.3 mg, 0.044 mmol) and methyl ethyl ketone (7 mL) were placed in a 25 mL screw-cap glass vial. The vial was heated for 11.5 h at 65 °C in an oven while being rotated at 18 rpm. The polymer was isolated by precipitation in pentane, purified by precipitation from THF into pentane four times and then dried to constant weight in a vacuum oven to afford 0.27 g (54% yield) of PNIPAM as a white powder. $M_{n,\,GPC}$ = 28.9 kDa, PDI = 2.00.

2.1.4 Polymer Characterization. Average molecular weights and molecular weight distributions were determined by GPC on a Waters GPC system consisting of a

Waters 515 HPLC pump, a Waters 717plus Autosampler, three Waters Styragel columns (HR2, HR3 and HR4; 30 cm × 7.8 mm; 5 μm particles; exclusion limits: 500-20,000, 500-30,000 and 5,000-600,000 g/mol, respectively) maintained at 40 °C and a Waters 2414 refractive index detector maintained at 35 °C. THF containing 0.25% (w/v) tetrabutylammonium bromide was used as the mobile phase (0.8 mL/min) and the system was calibrated with narrow-disperse polystyrene standards.

^{1}H NMR spectra were measured on Bruker AV 200 or DRX 500 spectrometers with samples dissolved in D_2O.

Samples for matrix-assisted laser desorption ionization-time-of-flight (MALDI–TOF) analysis were prepared by combining THF solutions of dithranol (20 mg/mL), PNIPAM (10 mg/mL), and sodium acetate (10 mg/mL) in a 10:1:1 ratio. MALDI-TOF spectra were acquired with a Micromass TofSpec 2E (20 kV operating voltage, 337 nm N_2 laser) in linear or reflectron mode. MALDI-quadrupole time-of-flight (QTOF) spectra were collected on a Micromass Global Ultima (9.1 kV operating voltage, 337 nm N_2 laser, MALDI mode) in reflectron mode.

Cloud points were measured on a Cary 100 Bio UV-vis spectrophotometer equipped with a temperature-controlled, six-position sample holder. Aqueous PNIPAM solutions (1 wt %) were heated at 0.2 °C/min while both the transmittance at 500 nm (1 cm path length) and the solution temperature, as determined by the internal temperature probe, were monitored.

A TA Instruments DSC 2910 differential scanning calorimeter (DSC) was used to measure the phase transition temperature of 1 wt % PNIPAM solutions (≈30 μL) in

hermetic aluminum crimp-seal pans while scanning at 1 °C/min. The temperatures of both the onset and maximum of the endotherm were determined. The DSC was calibrated with an indium standard for temperature and enthalpy changes.

2.2 Results and Discussion

2.2.1 Solvent Effect on ATR Polymerization of NIPAM. Alcohols were chosen as the solvents for ATRP on the base of the premise that a hydrogen-bonding solvent could bind to the amide groups of both monomer and polymer and thus reduce their interaction with both catalyst and propagating chain end. A similar approach had been used successfully in the ATRP of other strongly coordinating monomers, DMA[40] and 4-vinylpyridine.[42] Alcohols can dissolve many monomer/polymer and catalyst systems, and range widely in their hydrogen-bonding ability and polarity, permitting optimization of the polymerization. In this work, we explored ATRP of NIPAM in five alcohols: methanol, ethanol, 1-propanol, 2-propanol, and *tert*-butyl alcohol.

Monomer conversion and polymer molecular weight were determined at different stages during each polymerization. Conversions for polymerizations carried out in MeOH and *t*-BuOH were measured by ^{1}H NMR spectroscopy, while others were determined gravimetrically. Polymer molecular weights (MWs) and polydispersity indices (PDIs) were determined by a GPC method as developed by Müller.[25] This method had been established to give reproducible results, though with MW values significantly higher than those obtained from MALDI-TOF analysis,[25] and, therefore, the MW values determined by GPC in our work were only used to reveal trends. More precise molecular weights

were determined using ^{1}H NMR spectroscopy by comparing the peak areas of the polymer isopropyl C-H signal at 3.9 ppm, with the methoxy signal at 3.8 ppm arising from the MCP initiator. The M_n values determined by either GPC ($M_{n,GPC}$) or NMR ($M_{n,NMR}$) increased in proportion to the monomer:initiator (M:I) ratio (Table 1), and $M_{n,NMR}$ values were in reasonably good agreement with theoretical values.

The results for ATRP of NIPAM in the five alcohols are summarized in Table 1 and Figure 1 and show increasing monomer conversion along the series of alcohols MeOH, EtOH, *n*-PrOH, *i*-PrOH, and *t*-BuOH. Polymerizations in methanol turned deep blue as soon as the initiator was added, indicating high Cu(II) concentrations. This polymerization reached a plateau in conversion after 2 h (Figure 1).

Table 1. Monomer Conversion, Molar Mass (M_n), and Polydispersity (M_w/M_n) Data for Atom Transfer Radical Polymerization (ATRP) of *N*-isopropylacrylamide (NIPAM) in Alcohols[a]

solvent	$[M]_0:[I]_0$ (M/solvent) (w/w)	time (h)	conv (%)	$M_{n,th}$[b]	$M_{n,GPC}$[c]	$M_{n,NMR}$[d]	M_w/M_n[c]
MeOH	100:1 (1/2)	7	32	3 600	3 800		1.13
EtOH	100:1 (1/2)	9.5	64	7 200	10 400		1.09
n-PrOH	100:1 (1/2)	6	66	7 500	12 000		1.07
i-PrOH	50:1 (1/2)	4	89	5 000	8 000	5 000	1.15
i-PrOH	100:1 (1/2)	7	91	10 300	17 300	8 400	1.13
i-PrOH	200:1 (1/2)	8	79	17 900	35 600	15 700	1.13
i-PrOH	200:1 (1/1)	4.5	78	17 600	44 200	16 400	1.14
i-PrOH	400:1 (1/2)	12	73	33 000	67 600	27 300	1.27
i-PrOH	400:1 (1/1)	5.6	72	32 500	67 600	26 500	1.16
t-BuOH	50:1 (1/2)	3	79	4 500	7 300	4 400	1.15
t-BuOH	100:1 (1/2)	4	76	8 600	14 300	6 700	1.16
t-BuOH	200:1 (1/2)	4	76	17 200	37 500	14 400	1.14

[a] Experimental conditions: typically 3 g of NIPAM; MCP:CuCl:Me_6TREN = 1:1:1; room temperature. [b] $M_{n,th} = M_{NIPAM}[NIPAM]_0 conv/[MCP]_0$ [c] From GPC in 0.25% (w/v) Bu_4NBr/THF. [d] From ^1H NMR spectroscopy (500 MHz) in D_2O, 25 or 30 °C.

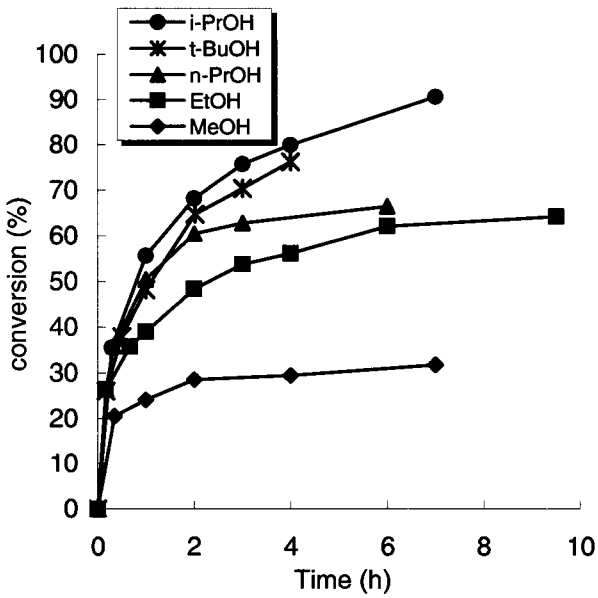

Figure 1. Monomer conversion vs. time curves for ATRP of NIPAM in different alcohols. Conditions: NIPAM:MCP:CuCl:Me_6TREN = 100:1:1:1; NIPAM:solvent = 1:2 (w/w); room temperature.

ATRP in EtOH and *n*-PrOH provided higher conversions, reaching ~ 65% after 6 h, but the first-order kinetic plots (Figure 2) show significant curvature. However, the low polydispersity index (PDI) at the end of polymerization shows that the growing centers were not lost, as this would have led to a much broader MW distribution. Therefore, the apparent curvature of the first-order kinetic plots is attributed to a progressive reduction of the concentration of the available catalyst. Analogous behavior has been observed for this initiating system during the ATRP of DMA in toluene.[33,34] Hence, while MCP/CuCl/Me_6TREN appears to be an efficient initiating system in a range of solvents, the catalyst deactivation is significant during the polymerization of acrylamides in EtOH and *n*-PrOH.

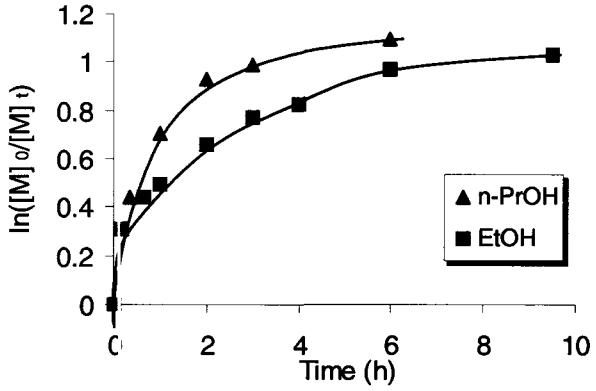

Figure 2. Kinetic plot for the ATRP of NIPAM in EtOH and *n*-PrOH. Conditions: NIPAM/ROH = 1/2 (w/w); NIPAM:MCP:CuCl:Me_6TREN = 100:1:1:1; room temperature.

In contrast, the higher branched alcohols *i*-PrOH and *t*-BuOH gave conversions of over 75% for target DPs of 50, 100, and 200 (Table 1). First-order kinetic plots (Figures 3A and 4A) show noticeable curvature, especially in the early stage of polymerization, resulting in an intercept in the kinetic plot. This could be attributed to fast activation but insufficient deactivation at the beginning of polymerization, so the polymerization proceeds too fast initially and leads to some radical termination.[30a,43] Addition of a small amount of Cu(II) species (~5% of Cu(I)) initially can enhance the deactivation reaction, reduce the intercept and improve the control of molecular weight and polydispersity.[31,44]

Therefore, several polymerizations were conducted in *i*-PrOH at M:I = 50:1, with 5, 10, or 20% of the CuCl replaced by $CuCl_2$. The rate of polymerization decreased as 5,

10 and 20% Cu(II) was added and high conversions were still achieved, however, there was no change in the apparent intercept (Figure 5).

In the polymerizations without the addition of Cu(II), the PDI remains narrow, and polymer MW increases linearly with conversion (Figures 3B and 4B),

The low PDI and the linearity in MW growth vs. conversion, along with the results obtained from the addition of Cu(II), indicate again that the curvature is due to progressive catalyst deactivation rather than chain termination. The catalyst deactivation is significantly diminished in these branched alcohols, although still not eliminated.

Polymerizations in *t*-BuOH became extremely viscous at high conversions, making sampling of high-MW polymers more difficult than in *i*-PrOH reactions at similar conversions.

Targeting higher molecular weights (M:I = 400) in *i*-PrOH gave lower conversions (~70%), a distinctly nonlinear kinetic plot (not shown), and a low molecular weight tail in the GPC (PDI = 1.27). Control was reestablished by increasing the initial monomer concentration from 33% to 50 wt %, which also resulted in faster polymerizations.

A

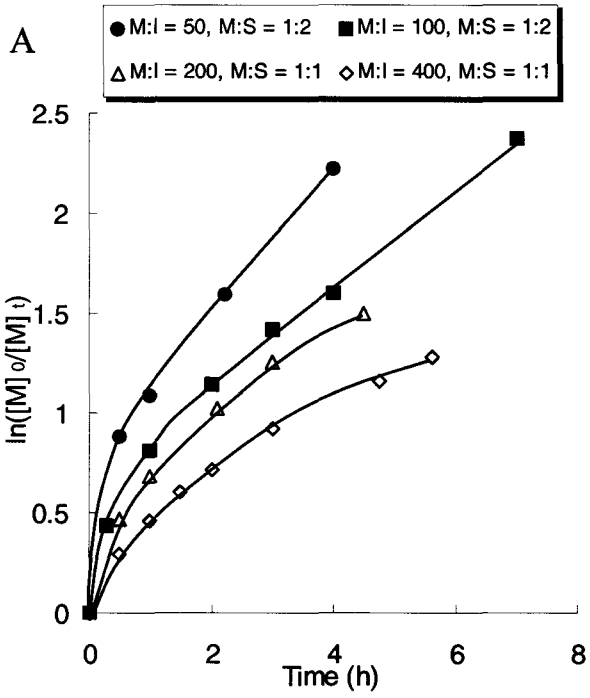
M:I = 50, M:S = 1:2
M:I = 100, M:S = 1:2
M:I = 200, M:S = 1:1
M:I = 400, M:S = 1:1
ln([M]o/[M]t)
Time (h)

B

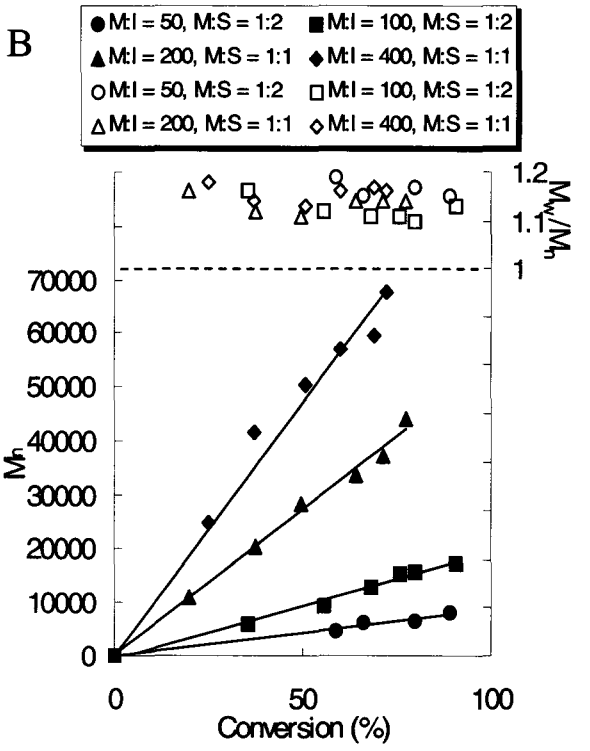
M:I = 50, M:S = 1:2
M:I = 100, M:S = 1:2
M:I = 200, M:S = 1:1
M:I = 400, M:S = 1:1
M:I = 50, M:S = 1:2
M:I = 100, M:S = 1:2
M:I = 200, M:S = 1:1
M:I = 400, M:S = 1:1
Mn
Mw/Mn
Conversion (%)

Figure 3. (A) Kinetic plot for the ATRP of NIPAM in *i*-PrOH. (B) Dependence of molecular weight ($M_{n,GPC}$) and polydispersity (M_w/M_n) on conversion. Conditions: NIPAM/*i*-PrOH = 1/2 or 1/1 (w/w); MCP:CuCl:Me_6TREN = 1:1:1; room temperature. The lines in (A) serve as guides for the eye while those in (B) are best-fit lines.

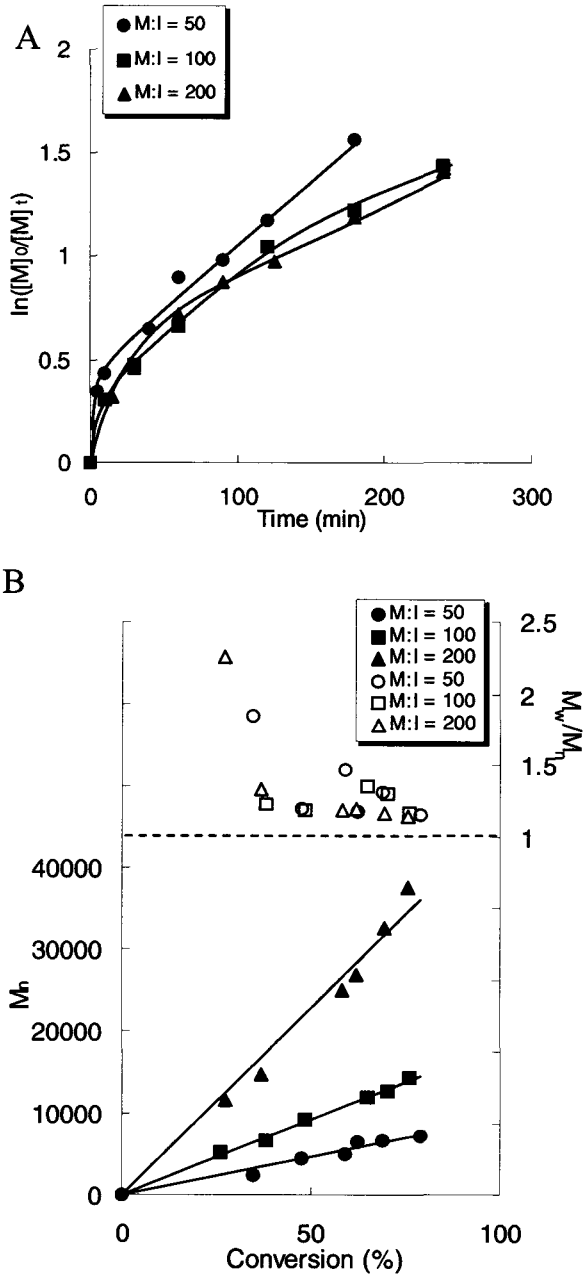

Figure 4. (A) Kinetic plot for the ATRP of NIPAM in *t*-BuOH. (B) Dependence of molecular weight ($M_{n,GPC}$) and polydispersity (M_w/M_n) on conversion. Conditions: NIPAM/*t*-BuOH = 1/2 (w/w); MCP:CuCl:Me_6TREN = 1:1:1; room temperature. The lines in (A) serve as guides for the eye while those in (B) are best-fit lines.

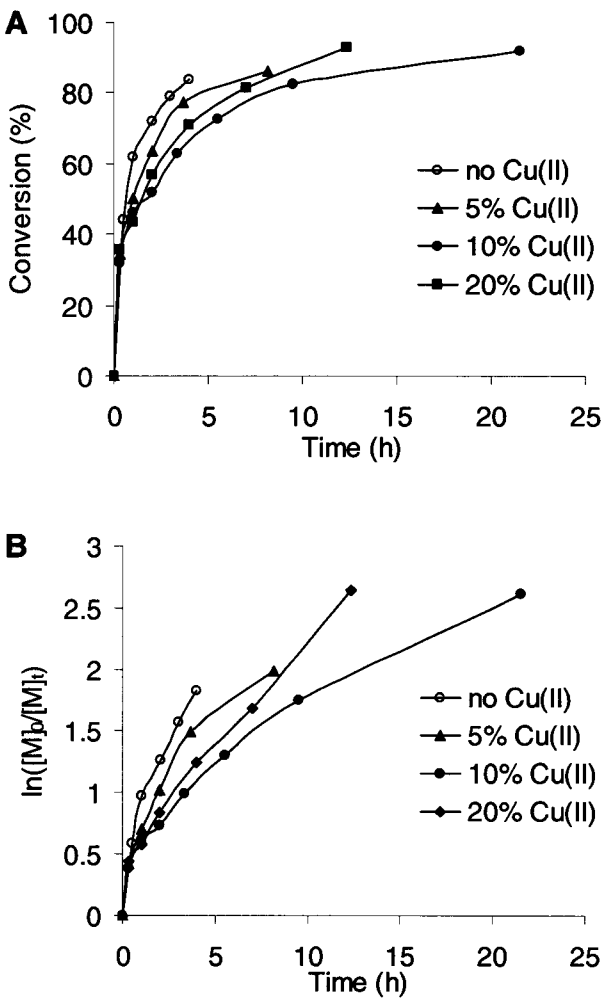

Figure 5. (A) Monomer conversion vs. time curves (B) Kinetic plot for the ATRP of NIPAM in *i*-PrOH with and without $CuCl_2$. Conditions:

NIPAM:MCP:CuCl+$CuCl_2$:Me_6TREN = 100:1:1:1; NIPAM:*i*-PrOH = 1:2 (w/w); room temperature.

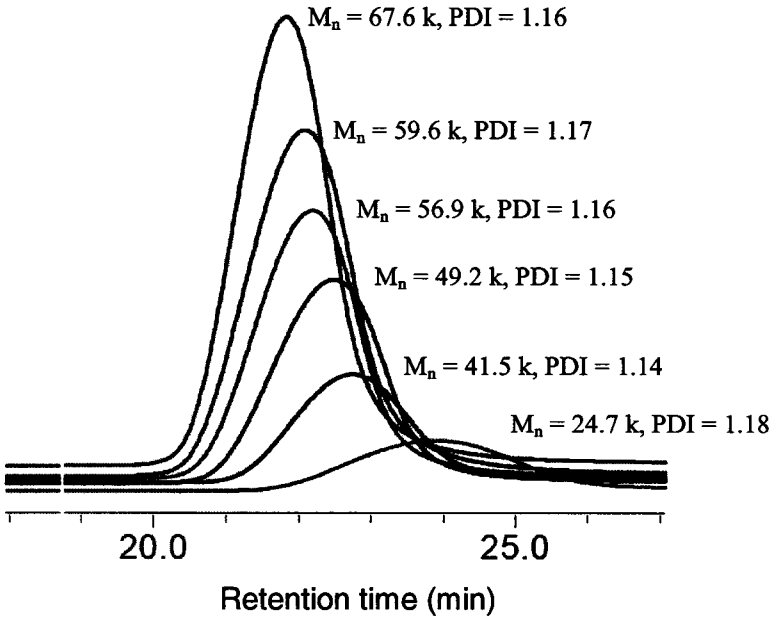

Figure 6. GPC traces of the ATRP of NIPAM in *i*-PrOH showing the evolution of molecular weight with time. Conditions: NIPAM/*i*-PrOH = 1/1 (w/w); NIPAM:MCP:CuCl:Me_6TREN = 400:1:1:1; room temperature.

2.2.2 PNIPAM Chain Extension. The living nature of the ATRP was confirmed by chain extension experiments. ATRP of NIPAM (M:I = 50:1) in *i*-PrOH was carried out for 4 h to 80% conversion, before adding another equivalent of NIPAM dissolved in i-PrOH such that the total M:I was 100:1. The polymerization was continued for another 6 h leading to a total conversion of 65%, corresponding to a conversion of

only 50% during the chain extension, but the PDI remained low (1.15). In contrast, addition of another equivalent of catalyst with the second portion of NIPAM raised the total conversion to 78% after 6 h, corresponding to 76% for the chain extension. Figure 7 shows the GPC traces of the PNIPAM chain extension experiment with additional catalyst, indicating a molecular weight increase consistent with conversion, and a narrow PDI. There is a small low MW shoulder indicating some termination takes place during the second monomer addition.

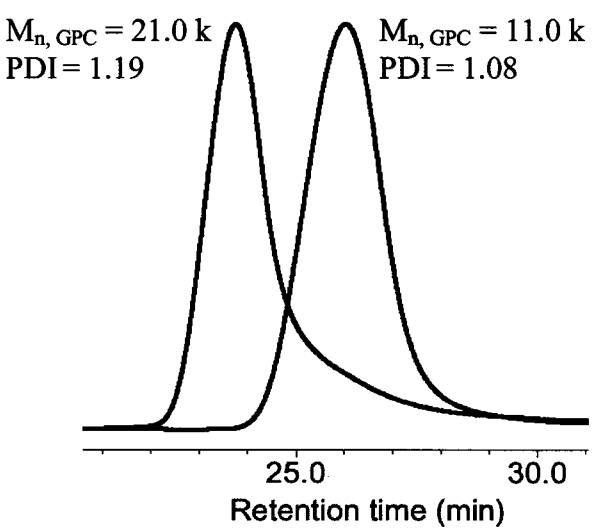

Figure 7. Gel permeation chromatograms for PNIPAM made a) with M:I = 50:1 (80% conversion) and b) by chain extension of the polymer with additional equivalents of both NIPAM and catalyst (total M:I = 100:1, total conversion = 78%).

These observations support the idea that catalyst deactivation, not loss of end group, causes the apparently nonlinear kinetics.

2.2.3 Mass Spectrometric Analysis of Molecular Weight and Chain Ends. PNIPAM samples were prepared in *i*-PrOH or *t*-BuOH with good conversions, controlled MWs and low PDIs. MALDI-TOF mass spectrometry was used to examine some of these polymers to confirm the MW and PDI, and identify the end groups, in analogy with previous studies.[32,35,45-48] We focused on lower MW samples (<10 kDa) since larger samples gave weak or nonexistent signals. Similar end groups were observed for PNIPAM samples made in *i*-PrOH or *t*-BuOH, and we believe that many of the observed end groups are due to the MALDI ionization process rather than the polymerization, as discussed below.

The MALDI-TOF mass spectrum of a PNIPAM sample prepared in *t*-BuOH (M:I = 50:1, entry 10 in Table 1) is shown in Figure 8. Figure 8A shows an envelope of peaks centered at 4000 Da and extending from 1000 to 7000 Da. These MALDI data give M_n = 4000 Da, similar to that determined by NMR (4500 Da) but, as expected,[25] less than that estimated by GPC (7250 Da). The MALDI PDI value of 1.08 for this sample is lower than the 1.15 measured by GPC, but confirms that the sample has a narrow MW distribution. The expanded spectrum (Figure 8B), reveals a repeating set of four peaks separated from neighboring sets by the monomer molecular weight (113 Da). The four peaks are attributed to chains bearing a methyl propionate (MePr) residue at one end, and an H, ene, OH, Cl or a lactone residue at the other end. For instance, the peak at m/z = 3844.0 corresponds to MePr-$(NIPAM)_{33}$-H/Na^+ (3845.3 calcd) and/or its unsaturated analog (3843.3 calcd). The peaks at m/z = 3861.6 and 3880.2, correspond to MePr-$(NIPAM)_{33}$-OH/Na^+ (3861.3 calcd) and MePr-$(NIPAM)_{33}$-Cl/Na^+ (3879.8 calcd),

respectively. The final peak at m/z = 3802.7 was assigned to a chain of DP = 33 that had undergone a cyclization to form a lactone end group (3802.3 calcd) as shown in Scheme 2.

Scheme 2

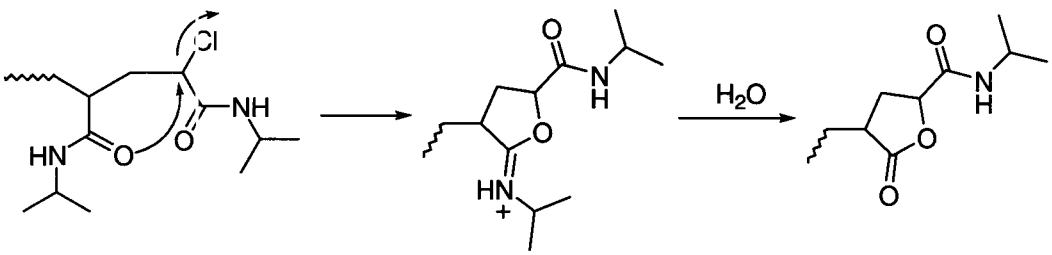

Figure 8C shows part of a higher resolution MALDI-quadrupole time-of-flight (QTOF) spectrum for the same sample. The region shown is for chains with DP = 22 and the isotopic pattern for each species is clearly resolved. The major set of peaks, centered at m/z = 2556.9, is now due to the lactone-terminated chain rather than the H-terminated one, likely the result of a small difference in the ionization process between the two experiments. This points to the difficulties in using the apparent end group chemistry as determined by MALDI-TOF to draw conclusions about the ATRP. The set of peaks due to the H-terminated chain, beginning at 2599.0, reveals the presence of a species with *m/z* 2 mass units lower, presumably the unsaturated analogue.

While H- and ene-terminated chains may result from disproportionation during polymerization, halogen-terminated polymer chains are known to form H, OH, ene and lactone end groups during mass spectrometric analysis[32,45-48] and similar processes occur during MALDI-TOF analysis of dithioester-terminated PNIPAM made by RAFT.[25] In addition, termination during PNIPAM polymerization is believed to occur by coupling

rather than disproportionation,[25] and peaks for the coupled product, MePr-(NIPAM)$_{33}$-MePr/Na^+ (3931.3 calcd), are weak or nonexistent. Lactone or related end groups are thought to occur during mass spectrometric analysis of poly(methyl methacrylate)[45,47,48] and PDMA[32] prepared by ATRP. Thus, the H, OH, ene and lactone end groups detected for PNIPAM in this work are believed to be formed during ionization in the mass spectrometer rather than during polymerization or subsequent handling. The MALDI-TOF results are hence consistent with a PNIPAM sample composed principally of chains bearing one MePr and one chloro end group and provide further evidence that the ATRP of NIPAM was successful, producing narrow-disperse PNIPAM with well-defined end groups.

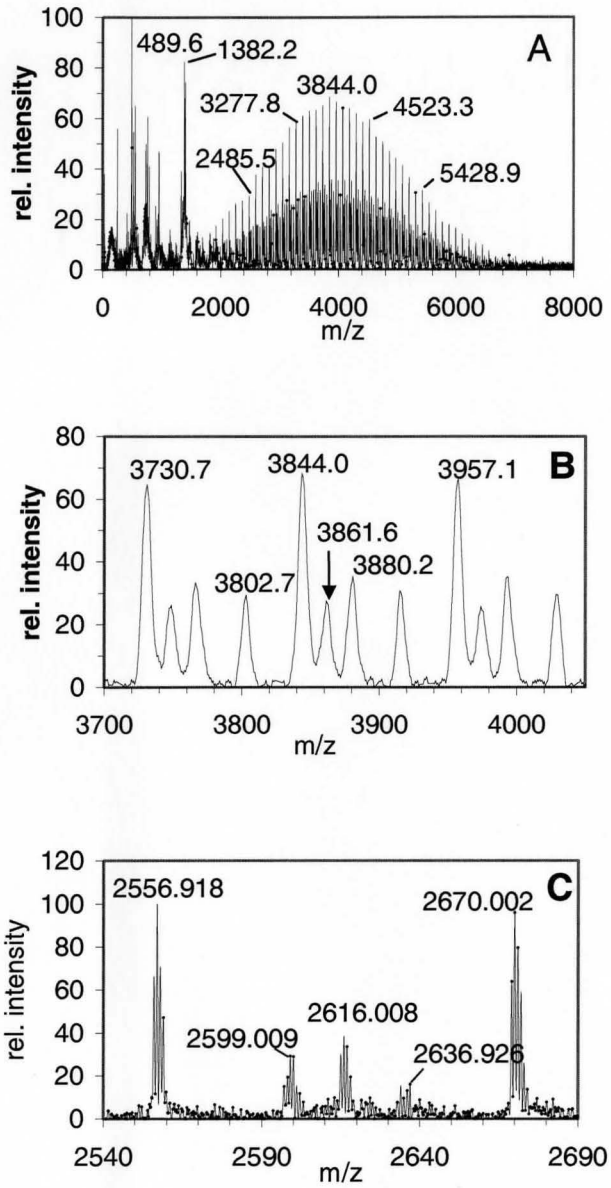

Figure 8. A) MALDI-TOF spectra for PNIPAM sample made in *t*-BuOH (M:I = 50:1, entry 10 in Table 1); B) expansion of spectrum **A** showing chains with DP = 32-34, C)

MALDI-QTOF spectrum of the same sample showing isotopic pattern for macromolecular species with DP =22.

2.2.4 Effect of Polymer MW on Thermal Phase Transitions. DSC and turbidimetry were used to measure endotherms and cloud points, respectively, for 1 wt % aqueous solutions of the PNIPAMs prepared by ATRP. Figure 9A shows a DSC trace obtained upon heating a 1 wt % solution of PNIPAM with $M_{n,NMR}$ = 6.5 kDa and PDI = 1.09. Heating rates of 1 °C/min were used in order to obtain reasonably strong endotherms, given the small sample volumes of 30 μL chosen to minimize thermal lag.

Figure 9B shows the transmittance vs temperature plots (cloud point curves) for PNIPAM with $M_{n,NMR}$ ranging from 2.8 to 26.5 kDa obtained with a heating rate of 0.2 °C/min. Also shown in Figure 9B is the cloud point curve for a polydisperse PNIPAM sample prepared by conventional free radical polymerization ($M_{n,GPC}$ = 28.9 kDa). While the transitions are quite sharp for samples with higher MW, they broaden for the lower MW samples, and the transition for the 2.8 kDa sample (curve a in Figure 9B) occurs over a >10 °C range. We attribute the early onset and broad transition observed with the 2.8, 5.0 (not shown) and 6.5 kDa samples to the hydrophobic MePr end groups on the residual low MW fractions present in these PNIPAMs. We hence use the 50% turbidity points (50%T) to interpret the polymer MW effect on the LCST, and the 90%T point to reflect contributions from the hydrophobic end groups. This is discussed in more detail below. The DSC and turbidimetry results are summarized in Table 2 and show reasonable agreement.

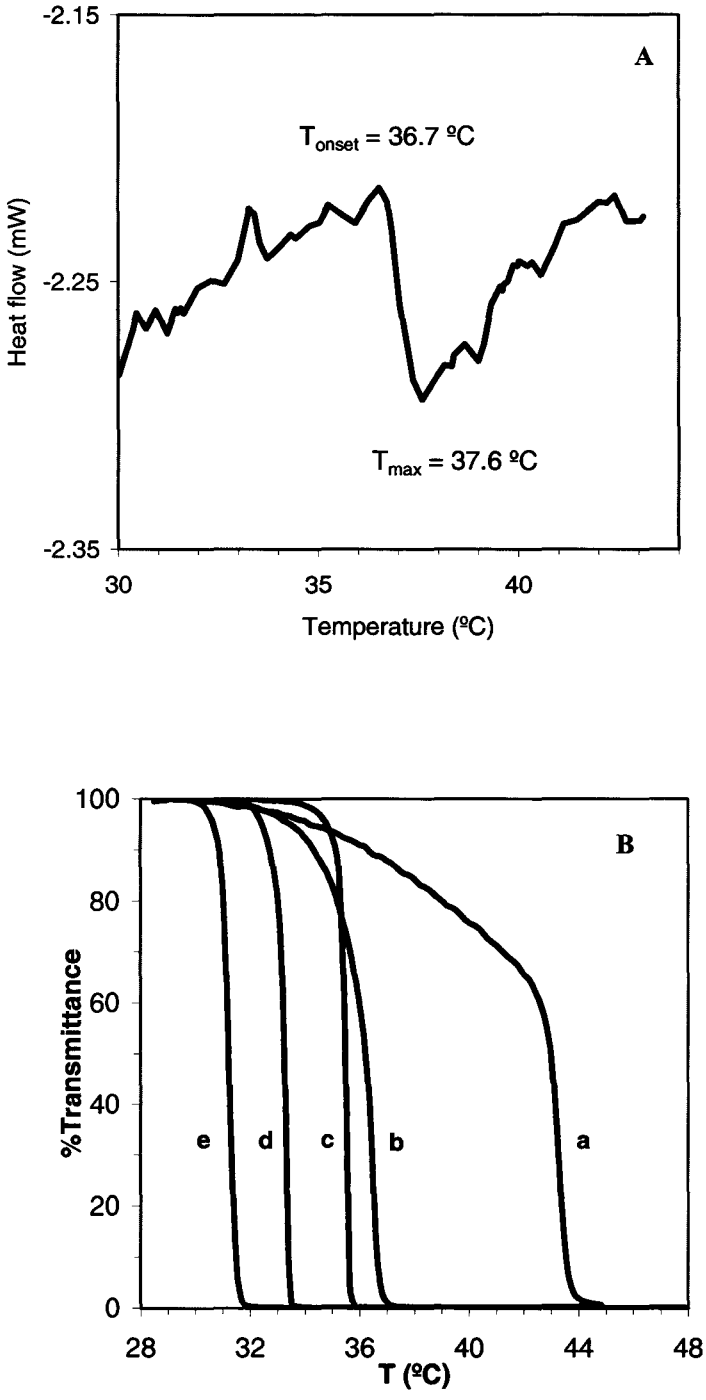

Figure 9. A) DSC thermogram for 1 wt% solution of PNIPAM sample with $M_{n,NMR}$ = 6.5 kDa and PDI = 1.09. Heating rate = 1.0 °C/min. B) Transmittance vs. temperature for 1

wt% solutions of PNIPAM made by a)-d) ATRP or e) conventional free-radical polymerization: $M_{n,NMR}$ = a) 2.8, b) 6.5, c) 10.9, d) 26.5 and e) $M_{n,GPC}$ = 28.9 kDa. Heating rate = 0.2 °C/min.

Table 2. Phase Transition Temperature of PNIPAM as a Function of Molecular Weight.

$M_{n,th}$ (kDa)	$M_{n,NMR}$ (kDa)	PDI[a]	phase transition temperature (°C)	
			turbidity[b] (90/50%T)	DSC[c] (onset/max)
3.3	2.8	1.07	36.3/43.0	43.3/47
5.0	5.0	1.15	37.5/38.9	39.7/41.7
7.0	6.5	1.09	34.3/36.3	36.7/37.6
8.6	6.7	1.16	36.1/36.4	36.5/38.2
13.2	10.9	1.11	35.1/35.5	35.6/36.4
17.9	15.7	1.13	34.4/34.6	34.7/35.5
32.5	26.5	1.16	32.7/33.3	33.5/34.4
--[d]	28.9[d]	2.00	30.8/31.2	29.3/31.6

a) Measured by GPC. b) 1 wt% solution; heating rate = 0.2 °C/min. c) 1 wt% solution; heating rate = 1.0 °C/min. d) Prepared by conventional free radical polymerization. M_n measured by GPC.

This is to our knowledge the first study into the effect of MW on cloud point using narrow-disperse PNIPAM. As the MW ($M_{n,NMR}$) increases from 2.8 to 26.5 kDa, the cloud point (50% T) drops from 43.0 to 33.3 °C and approaches the range of 31-32 °C commonly reported for PNIPAM (Figure 10). Interestingly, a PNIPAM sample made by conventional free radical polymerization with AIBN initiator had $M_{n,GPC}$ = 28.9 kDa (note: GPC likely overestimates M_n by a factor of two) and PDI = 2.0 and gave a cloud point of 31.2 °C. This falls within the typical range, but is about 3 °C lower than a narrow-disperse

sample of similar M_n made by ATRP. This is attributed to the significant high MW fraction present in such polydisperse samples. This fraction will have a lower LCST and thus may mask the transition of the major, but lower MW, fraction. This illustrates the importance of using narrow-disperse polymers in studies of LCST behavior.

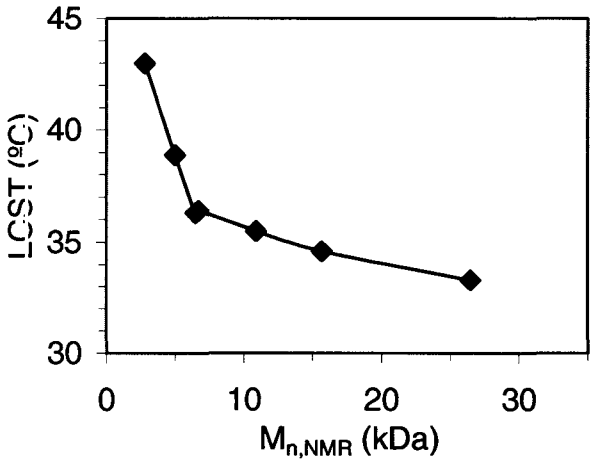

Figure 10. Cloud point (50% T) vs. polymer molecular weight ($M_{n,NMR}$) for narrow-disperse PNIPAM samples made by ATRP. Cloud points determined by turbidimetry on 1 wt % solutions, heating rate = 0.2 °C/min.

As mentioned earlier, previous studies of PNIPAM and other thermoresponsive polymers have found the LCST to be independent,[5,14,15] directly dependent,[8,22] or inversely dependent[6,16-21] upon MW. LCSTs are expected to decrease with increasing polymer MW on the basis of the changes in the polymer-solvent interaction.[16,49] However, end groups derived from initiators, terminators or chain-transfer agents can mitigate this

trend, especially at lower MWs, by changing the hydrophobic/hydrophilic nature of the polymer. It was found that LCSTs were decreased by hydrophobic end groups and increased by hydrophilic end groups, with the magnitude of the effect depending on the nature of the end group. [14,22,50,51]

Thus, the MW effect on LCST should be seen as a combination of changes in polymer-solvent interaction, along with changes in the importance of end group contributions to the hydrophobic/hydrophilic balance of the polymer. The improved control over end groups possible with ATRP should make it possible to begin to resolve these two effects.

The PNIPAM studied in this work bears MePr and chloro end groups. Methyl propionate itself is weakly hydrophobic (6.4 wt % solubility in water at 20 °C)[52] and does not appear to have a significant effect on the cloud points of the higher MW polymers studied here. However, in oligomeric PNIPAM, the MePr end group could perturb the hydrophobic/hydrophilic balance enough to show a lower onset of the cloud point, seen most clearly in the 90% T data. In fact, we attribute the early onset and low-temperature slopes observed in the turbidity curves of the 2.8, 5.0 and 6.5 kDa samples (see Figure 9B) to the MePr end group. These low MW samples will possess significant oligomeric fractions less than 1 kDa, which would be sensitive to the hydrophobic effect of the MePr end group and show early phase separation seen in 90%T. We plan to test this hypothesis by preparing oligomeric PNIPAM samples bearing MePr end groups. Given the low hydrophobicity of the MePr end group we believe this to be a minor effect that would not distort MW influence on the cloud point seen in the 50%T data.

Studies aimed at further probing the effect of a range of different end groups on the cloud points of PNIPAMs of different MWs are underway and will be reported in the near future.

2.3 Conclusion

We have shown that ATRP of NIPAM in *i*-PrOH and *t*-BuOH leads to narrow-disperse PNIPAM with high conversion and good molecular weight control. These branched alcohols are thought to hydrogen-bond to monomer and polymer, thereby reducing the known deactivation of the ATRP catalyst by acrylamides and their polymers.

Aqueous solutions of these PNIPAMs showed a dramatic decrease in cloud point with increasing MW, attributed to the reduced entropy of mixing with increasing MW.

In addition, the lowest MW samples showed an early onset of phase separation, which is attributed to the presence of oligomer that is influenced more strongly by the slightly hydrophobic MePr end group.

Hence, the use of ATRP to prepare PNIPAMs allows good control over both polymer MW and end group, an ability that is being exploited in our current work to prepare PNIPAMs with a range of end groups of different polarity in order to study their effects on the LCST.

References

(1) Heskins, M.; Guillet, J. E. *J. Macromol. Sci. Chem.* **1968**, *A2*, 1441-1455.

(2) Schild, H. G. *Prog. Polym. Sci.* **1992**, *17*, 163-249.

(3) Chen, G.; Hoffman, A. S. *Nature* **1995**, *373*, 49-52.

(4) Hay, D. N. T.; Rickert, P. G.; Seifert, S.; Firestone, M. A. *J. Am. Chem. Soc.* **2004**, *126,* 2290-2291.

(5) Fujishige, S.; Kubota, K.; Ando, I. *J. Phys. Chem.* **1989**, *93,* 3311-3313.

(6) Schild, H. G.; Tirrell, D. A. *J. Phys. Chem.* **1990**, *94,* 4352-4356.

(7) Cho, E. C.; Lee, J.; Cho, K. *Macromolecules* **2003**, *36*, 9929-9934.

(8) Tong, Z.; Zeng, F.; Zheng, X.; Sato, T. *Macromolecules* **1999**, *32*, 4488-4490; Zheng, X.; Tong, Z.; Xie, X.; Zeng, F. *Polym. J.* **1998**, *30*, 284-288.

(9) Winnik, F. M.; Ringsdorf, H.; Venzmer, J. *Macromolecules* **1990**, *23*, 2415-2416.

(10) Schild, H. G.; Muthukumar, M.; Tirrell, D. A. *Macromolecules* **1991**, *24*, 948-952.

(11) Otake, K.; Karaki, R.; Ebina, T.; Yokoyama, C.; Takahashi, S. *Macromolecules* **1993**, *26*, 2194-2197.

(12) Schild, H. G.; Tirrell, D. A. *Langmuir* **1991**, *7,* 665-671.

(13) Lee, L. T.; Cabane, B. *Macromolecules* **1997**, *30*, 6559-6566.

(14) Otake, K.; Inomata, H.; Konno, M.; Saito, S. *Macromolecules* **1990**, *23*, 283-289.

(15) Tiktopulo, E. I.; Uversky, V. N.; Lushchik, V. B.; Klenin, S. I.; Bychkova, V. E.; Ptitsyn, O. B. *Macromolecules* **1995**, *28*, 7519-7524.

(16) Lessard, D. G.; Ousalem, M.; Zhhgu, X. X. *Can. J. Chem.* **2001**, *79*, 1870-1874.

(17) Xue, W.; Huglin, M. B.; Jones, T. G. J. *Macromol. Chem. Phys.* **2003**, *204*, 1956-1965.

(18) Kunugi, S.; Tada, T.; Tanaka, N.; Yamamoto, K.; Akashi, M. *Polym. J.* **2002**, *34*, 383-388.

(19) Aoshima, S.; Oda, H.; Kobayashi, E *J. Polym. Sci. A: Polym. Chem.* **1992**, *30*, 2407-2413.

(20) Laukkanen, A.; Valtola, L.; Winnik, F. M.; Tenhu, H. *Macromolecules* **2004**, *37*, 2268-2274.

(21) Bütün, V.; Armes, S. P.; Billingham, N. C. *Polymer* **2001**, *42*, 5993-6008.

(22) Liu, Q.; Yu, Z.; Ni, P. *Colloid Polym. Sci.* **2004**, *282*, 387-393.

(23) Chiefari, J.; Chong, Y. K.; Ercole, F.; Kristina, J.; Jeffery, J.; Le, T. P. T.; Mayadunne, R. T. A.; Meijs, G. F.; Moad, C. L.; Moad, G.; Rizzardo, E.; Thang, S. H. *Macromolecules* **1998**, *31*, 5559-5562.

(24) Ganachaud, F.; Monteiro, M. J.; Gilber, R. G.; Dourges, M.; Thang, S. H.; Rizzardo, E. *Macromolecules* **2000**, *33*, 6738-6745.

(25) Schilli, C.; Lanzendörfer, M. G.; Müller, A. H. E. *Macromolecules* **2002**, *35*, 6819-6827.

(26) Ray, B.; Isobe, Y.; Matsumoto, K.; Habaue, S.; Okamoto, Y.; Kamigaito, M.; Sawamoto, M. *Macromolecules* **2004**, *37*, 1702-1710.

(27) Convertine, A. J.; Ayres, N.; Scales, C. W.; Lowe, A. B.; McCormick, C. L. *Biomacromolecules* **2004**, *5*, 1177-1180.

(28) Hawker, C. J.; Bosman, A. W.; Harth, E. *Chem. Rev.* **2001**, *101*, 3661-3688.

(29) Bosman, A. W.; Vestberg, R.; Heumann, A.; Fréchet, J. M. J.; Hawker, C. J. *J. Am. Chem. Soc.* **2003**, *125*, 715-728.

(30) (a) Matyjaszewski, K.; Xia, J. *Chem. Rev.* **2001**, *101*, 2921-2990. (b) Kamigaito, M.; Ando, T.; Sawamoto, M. *Chem. Rev.* **2001**, *101*, 3689-3746.

(31) Teodorescu, M.; Matyjaszewski, K. *Macromolecules* **1999**, *32*, 4826-4831.

(32) Rademacher, J. T.; Baum, M.; Pallack, M. E.; Brittain, W. J.; Simonsick, W. J. *Macromolecules* **2000**, *33*, 284-288.

(33) Teodorescu, M.; Matyjaszewski, K. *Macromol. Rapid Commun.* **2000**, *21*, 190-194.

(34) Neugebauer, D.; Matyjaszewski, K. *Macromolecules* **2003**, *36*, 2598-2603.

(35) Masci, G.; Giacomelli, L.; Crescenzi, V. *Macromol. Rapid Commun.* **2004**, *25*, 559-564.

(36) Jones, J. A.; Novo, N.; Flagler, K.; Pagnucco, C. D.; Carew, S.; Cheong, C.; Kong, X. Z.; Burke, N. A. D.; Stöver, H. D. H., *J. Polym. Sci. A: Polym. Chem.*, *submitted*; Jones, J.A. *M.Sc. Thesis*, McMaster University, 1999.

(37) Yin, X.; Stöver, H. D. H. *Macromolecules* **2002**, *35*, 10178-10181.

(38) Yin, X.; Stöver, H. D. H. *Macromolecules* **2003**, *36*, 9817-9822.

(39) Yin, X.; Stöver, H. D. H. *J. Polym. Sci. A: Polym. Chem.*, **2005**, *43*, 1641-1648.

(40) Yin, X.; Stöver, H. D. H. *Macromolecules*, **2005**, *38*, 2109-2115.

(41) Ciampolini, M.; Nardi, N. *Inorg. Chem.* **1966**, *5*, 41-44.

(42) Xia, J.; Zhang, X.; Matyjaszewski, K. *Macromolecules* **1999**, *32*, 3531-3533.

(43) Kajiwara, A.; Matyjaszewski, K.; Kamachi, M. *Macromolecules* **1998**, *31*, 5695-5701.

(44) Ding, S.; Radosz, M.; Shen, Y. *Macromol. Rapid Commun.* **2004**, *25*, 632-636.

(45) Barner-Kowollik, C.; Davis, T. P.; Stenzel, M. H. *Polymer* **2004**, *45*, 7791-7805.

(46) Nonaka, H.; Ouchi, M.; Kamigaito, M.; Sawamoto, M. *Macromolecules* **2001**, *34*, 2083-2088.

(47) Singha, N. K.; Rimmer, S.; Klumperman, B. *Eur. Polym. J.* **2004**, *40*, 159-163.

(48) Borman, C. D.; Jackson, A. T.; Bunn, A.; Cutter, A. L.; Irvine, D. J. *Polymer* **2000**, *41*, 6015-6020.

(49) Patterson, D. *Macromolecules* **1969**, *2*, 672-677.

(50) Chung, J. E.; Yokoyama, M.; Aoyagi, T.; Sakurai, Y.; Okano, T. *J. Controlled Release* **1998**, *53*, 119-130.

(51) Chung, J. E.; Yokoyama, M.; Suzuki, K.; Aoyagi, T.; Sakurai, Y.; Okano, T. *Colloids Surf. B: Biointerfaces* **1997**, *9*, 37-48.

(52) Solubility Data Series, Getzen, F.; Hefter, G.; Maczynski, A.; eds., Pergamon, Oxford, 1992, vol. 48, p. 138-147.

Appendix. ^{1}H NMR of PNIPAM

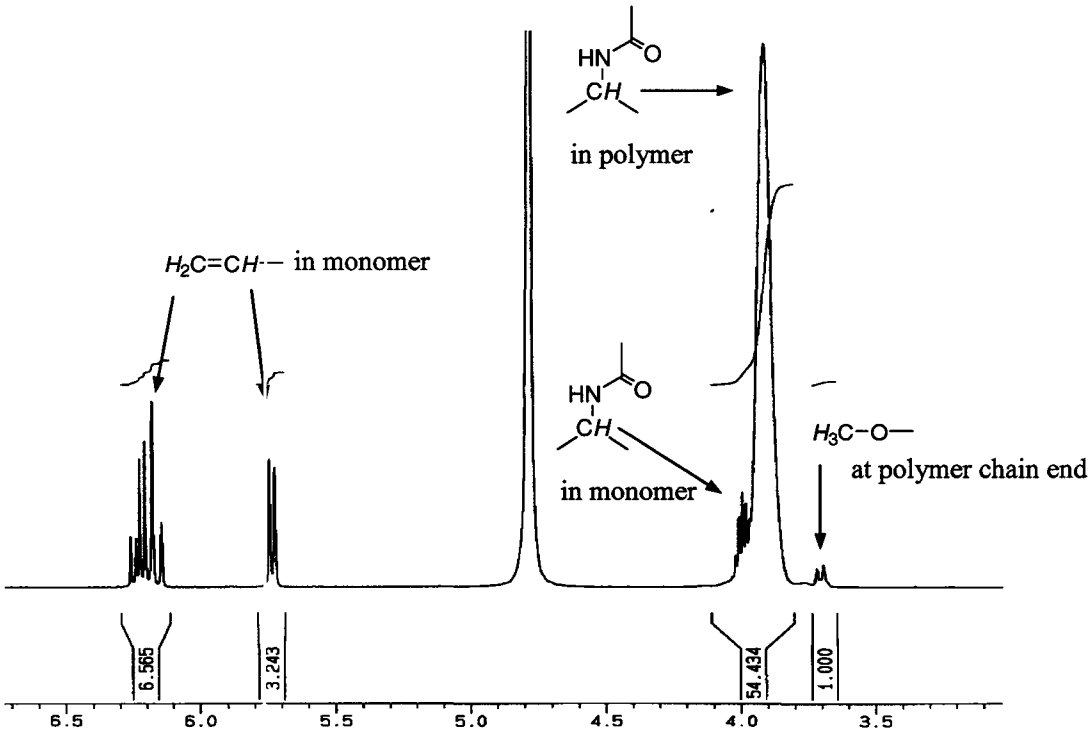

Figure 1. ^{1}H NMR spectrum of PNIPAM initiated by MCP (with NIPAM residual) in D_2O.

Chapter 3 The End Group Effect on the Thermal Response of Narrow-Disperse Poly(*N*-isopropylacrylamide) Prepared by Atom Transfer Radical Polymerization

Abstract

Four series of narrow-disperse poly(*N*-isopropylacrylamide) (PNIPAM) with well-controlled molecular weights and with end groups of varying hydrophobicity were synthesized by room temperature atom transfer radical polymerization in 2-propanol using the corresponding chloropropionate and chloropropionamide initiators. The thermal phase transitions of aqueous solutions of these PNIPAMs were studied by turbidimetry and high-sensitivity differential scanning calorimetry (HS-DSC). The four series of samples showed an inverse molecular weight (MW) dependence of their cloud point. The magnitude of the MW dependence decreases when using more hydrophobic end groups. The end groups were observed to have effects on the cloud point, on the shape of the cloud point curves, and on the enthalpy of the phase transition. Above the cloud point, narrow-disperse PNIPAM sedimented more rapidly than polydisperse PNIPAM produced by conventional free radical polymerization, especially at concentrations above 1%. Thus, multiple HS-DSC scans of PNIPAM prepared by ATRP typically gave repeatable results only at lower concentrations.

3.0 Introduction

The molecular weight (MW) dependence of the lower critical solution temperature (LCST) or the related cloud point of polymers has been an active yet

controversial topic. The LCSTs of poly(*N*-isopropylacrylamide) (PNIPAM) and related thermoresponsive polymers have been reported to be inversely dependent,[1-7] directly dependent,[8,9] or independent[10-12] on the molecular weight. However, most of these studies involved conventionally prepared, polydisperse polymers, which may have precluded precise examination of MW effects. In addition, different initiators, terminators or chain-transfer agents led to different polymer end groups, which can in turn affect the cloud points by changing its hydrophobic/hydrophilic balance.[9,11,13-16] Hydrophobic end groups decrease cloud points while hydrophilic end groups tend to increase them, with the magnitude of the effect depending on the nature of the end group. Hydrophobic groups act by increasing the degree of ordering of solvating water while hydrophilic ones tend to decrease the ordering of solvating water. These effects are believed to be greater for hydrophobic/hydrophilic groups located at chain ends rather than mid-chain.[13]

End group effects are most pronounced for low MW polymers but have also been reported for polymers with very high MWs. For example, Saito and coworkers studied several PNIPAM samples prepared with AIBN, and one prepared with persulfate initiator.[11] They found that the cloud point was constant at 31.5 °C for the AIBN-initiated PNIPAM samples for MW's ranging from 11 to 203 kDa, while the cloud point for the persulfate-initiated sample with MW = 2100 kDa was more than 2 °C higher, which was attributed to the sulfate chain ends in this sample.

In fact, the dependence of cloud point on polymer MW observed in some studies may be attributed, at least in part, to the role of the end group. Polymers with hydrophilic end groups, such as those derived from persulfate initiation or a hydrophilic chain transfer

agent, tend to show both higher cloud points, and cloud points that drop as the polymer MW increases. [2,4,6,12]

In contrast, polymers bearing hydrophobic end groups tend to have lower cloud points, that are either independent of polymer MW or increase with polymer MW. [8-12] Interestingly, intra- and intermolecular micellization can effectively isolate very hydrophobic groups from water, and hence dramatically suppress their hydrophobic effects. For example, alkyl-terminated PNIPAMs can form a hydrophobic core of alkyl chain ends and a diffuse corona of PNIPAM chains when the alkyl end group is long enough to facilitate the micellization.[13-15,17,18]

Therefore, contributions from the end groups have to be considered when studying the MW dependence of cloud points. Key questions, including how much different hydrophilic/hydrophobic end groups affect the cloud point of polymers with identical MW, and how much a single group affects the MW dependence of cloud points, still remain uncertain. This is largely due to the lack of control over both MW and end group chemistry for PNIPAM.

We recently succeeded in preparing narrow-disperse PNIPAMs by atom transfer radical polymerization (ATRP) and reported the MW dependence of their cloud points.[19] In contrast to previous studies, the aqueous solutions of these narrow-disperse PNIPAMs showed a dramatic decrease in cloud point with increasing MW. The MW dependence could be seen as a combination of MW and end group effects.

In the present work we take advantage of the simultaneous control over MW and end groups through choice of appropriate ATRP initiators, and are now able to

unambiguously resolve the effects of MW and end groups on the cloud points. We first describe the synthesis of narrow-disperse PNIPAMs with different end groups ranging from hydrophilic amide to hydrophobic phenylamide by ATRP using the corresponding initiators. This includes a polymer initiated using isopropyl 2-chloropropionamide, representing PNIPAM with a hydrogen atom at the initiation end and a chlorine at the termination end. We then report our study of the MW and end group effects on phase transitions of 1 % aqueous solutions of these PNIPAMs as determined by turbidimetry and microcalorimetry.

3.1 Experimental Section

3.1.1 Materials. *N*-Isopropylacrylamide (Aldrich, 97%) was recrystallized twice from benzene/hexane prior to use. Copper(I) chloride (97%), ethyl 2-chloropropionate (97%), 2-chloropropionamide (98%), isopropylamine (99.5+%), aniline (99%), triethylamine (99.5%), 2-chloropropionyl chloride (97%), and tetrabutylammonium bromide (99%) were purchased from Aldrich and used as received. Me_6TREN was prepared as described in the literature.[20] 2-Propanol (*i*-PrOH, Fisher, HPLC grade), *tert*-butyl alcohol (*t*-BuOH, Fisher, Certified), tetrahydrofuran (THF, Caledon, HPLC grade), pentane (Caledon, Reagent grade), methylene chloride (Caledon, Reagent grade), hexanes (Caledon, Reagent grade), and ethyl acetate (Fisher, 99.9%) were used as received.

3.1.2 Synthesis of *N*-Isopropyl-2-chloropropionamide. *N*-Isopropyl-2-chloropropionamide was synthesized by a modification of Brittain's method.[21] Isopropylamine (4 ml, 0.05 mol) and triethylamine (14 ml, 0.1 mol) were dissolved in 80

ml methylene chloride and cooled in an ice bath. After 15 min, 2-chloropropionyl chloride (5 ml, 0.05 mol) dissolved in 20 ml methylene chloride was added dropwise over 20 min. The reaction was stirred at 0 °C for 30 min and then at room temperature for 3 h. 30 ml 1 M HCl and three 30 ml aliquots of water were added to dissolve the salt formed during the reaction. The organic layer was washed with two 30 ml aliquots of 5% $NaHCO_3$ solution and dried over Na_2SO_4. The solvent was removed on a rotary evaporator to yield a deep yellow solid that was recrystallized three times from ethanol/water (7:5 v/v) and passed through a silica column to remove color, using hexane/ethyl acetate (10:1 v/v) as the eluent. The dried sample was recrystallized from ethanol/water and dried under vacuum to afford white crystals (2.9 g, 39% yield). ^{1}H NMR ($CDCl_3$): 6.3 ppm (bs, 1H, -N*H*CH$(CH_3)_2$), 4.35-4.39 ppm (m, 1H, -C*H*ClCH$_3$), 4.03-4.07 ppm (m, 1H, -C*H*$(CH_3)_2$), 1.72-1.73 ppm (d, 3H, -CHClC*H*$_3$), 1.18-1.20 (dd, 6H, -CH(C*H*$_3)_2$).

3.1.3 Synthesis of *N*-phenyl-2-chloropropionamide. The same procedure used for the synthesis of *N*-isopropyl-2-chloropropionamide was applied to synthesize *N*-phenyl-2-chloropropionamide, yielding a yellow solid. It was purified by recrystallization from ethanol/water (5:2 v/v) to give the product in 42% yield. ^{1}H NMR ($CDCl_3$): 8.2 ppm (bs, 1H, -N*H*C$_6$H$_5$), 7.15-7.56 ppm (m, 5H, -N*H*C$_6$H$_5$), 4.53-4.57 ppm (q, 1H, -C*H*ClCH$_3$), 1.83-1.84 ppm (d, 3H, - CHClC*H*$_3$).

3.1.4 General Procedure for ATRP of NIPAM. To prepare PNIPAM with a target degree of polymerization of 50, NIPAM (2.00 g, 17.7 mmol), CuCl (0.035 g, 0.35 mmol) and 2-propanol (4.00 g), deoxygenated by bubbling with nitrogen for at least 30

min, were combined and then transferred to a nitrogen-purged 25 mL round-bottom flask fitted with a septum. Me_6TREN (0.081 g, 0.35 mmol) was added via a nitrogen-purged syringe and the solution was stirred for 20 min to allow formation of the CuCl/Me_6TREN complex. The initiator (0.35 mmol), neat or as a concentrated solution in 2-propanol, was then added using a syringe to begin the polymerization. The reactions were carried out at room temperature under a slight positive pressure of nitrogen.

Aliquots (0.6 mL) were removed at regular intervals, divided between two vials in a 5:1 ratio, the larger portion accurately weighed and then both portions were dried under a stream of air. The smaller sample was dissolved in THF, passed through a short silica column to remove the catalyst, dried under a stream of air and used for gel permeation chromatography (GPC) analysis. The larger portion of the aliquot was used to determine conversion: The dried sample was first reprecipitated from THF into pentane (1:12 v/v), and dried to constant weight under vacuum at 60 °C. Conversion was then determined gravimetrically and corrected for residual monomer using ^1H NMR spectroscopy.

3.1.5 Preparation of PNIPAM Oligomer (Targeted Degree of Polymerization ≤ 10). PNIPAM oligomers were prepared following the same procedure as described for ATRP of NIPAM, except that *t*-butanol was used as the polymerization solvent. Ethyl chloropropionate was used as the initiator. In order to reduce the initial radical concentration and thus radical termination, a monomer:solvent ratio of 1:3 was used, and the amount of catalyst and ligand relative to initiator was halved, with monomer:initiator:CuCl:Me_6TREN = 20:2:1:1. Two independent polymerizations were conducted and stopped after 0.5 h and 4.6 h, at monomer conversions of 45% and 77%,

respectively. Two oligoNIPAM products were obtained and designated as, oligoNIPAM-4 and oligoNIPAM-10, respectively. As it was difficult to isolate the oligomers by precipitation from the oligomer/monomer reaction mixture, conversion was measured directly by ^{1}H NMR spectroscopy in D_2O after the sample was air-dried. Here, the peak areas of monomer signals at 5.7 (one proton) or 6.2 ppm (two protons) were compared with the polymer signal at 3.9 ppm (one proton), corrected for contributions due to the monomer.

For isolation, the dried sample dissolved in hexane/THF (5:1 v/v) and passed through a silica column. Monomer eluted first, and the desired oligomer was subsequently eluted using neat THF while the catalyst remained on the silica. The oligomer fractions were dried and redissolved in water, and then freeze-dried to yield white power. These were further dried to constant weight under vacuum at 60 °C.

3.1.6 Polymer Characterization. As in Chapter 2, Experimental section.

3.1.7 Determination of Phase Transitions in Aqueous Solutions. Cloud points were measured on a Cary 100 Bio UV-visible spectrophotometer equipped with a temperature-controlled, six-position sample holder. Aqueous PNIPAM solutions (1 wt %) were heated at 0.2 °C/min while both the transmittance at 500 nm (1 cm path-length) and the solution temperature, as determined by the internal temperature probe, were monitored.

HS-DSC was performed on a MicroCal VP-DSC microcalorimeter to measure the phase transition temperature of 1 wt % PNIPAM solutions. Samples were degassed and transferred to the 0.5121 ml sample cell (17×8×6.5 mm (h×w×l), Tantalum wall) by

syringe. Samples were scanned at a constant heating rate which was varied from 15 to 60 °C/h at an external pressure of 170 kPa. The sample cell was cleaned by flushing with 300 ml distilled water, then with 10 ml methanol, and finally with 600 ml distilled water to remove residual methanol. The DSC was calibrated by supplying a precisely known current to the reference cell of the microcalorimeter.

3.2 Results and Discussion

3.2.1 ATRP of NIPAM with Different Initiators. PNIPAMs with different end groups were synthesized by ATRP employing a series of initiators so as to produce end groups varying in hydrophobicity. ATRP of acrylamides has suffered from lack of control and from low conversions, mainly attributed to the competitive coordination of their amide groups with the metal catalysts.[21-24] In our previous studies of ATRP of DMA[25] and NIPAM,[19] we used alcohols as polymerization solvents on the hypothesis that they might protect the catalyst by hydrogen bonding to the amide groups of both monomer and polymer. ATRP of NIPAM in 2-propanol was found to give good control and high conversions,[19] and was hence used again in this work. 2-Chloropropionates and 2-chloropropionamides were used together with CuCl as catalyst and Me_6TREN as ligand at 1:1:1 ratios to initiate polymerizations, based on previous studies.[19,21-25] Specifically, 2-chloropropionamide (CP), isopropyl 2-chloropropionamide (*i*-PrCP), ethyl 2-chloropropionate (ECP), and phenyl 2-chloropropionamide (PhCP) were chosen as initiators to give polymers with end groups of varying polarity, ranging from hydrophilic for CP to hydrophobic for PhCP (Figure 1).

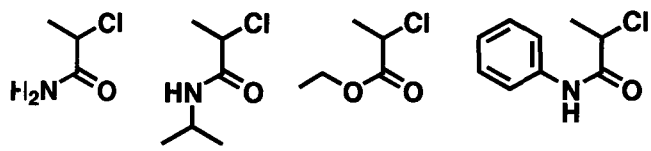

Figure 1. Chemical structures of 2-chloropropionamide (CP), isopropyl 2-chloropropionamide (*i*-PrCP), ethyl 2-chloropropionate (ECP), and phenyl 2-chloropropionamide (PhCP).

Monomer conversion and polymer molecular weight were determined at different stages during each polymerization. Conversions were determined gravimetrically. Polymer molecular weights (MWs) and polydispersity indices (PDIs) were determined by a GPC method developed by Müller.[26] This method had been established to give reproducible results, though with MW values significantly higher than those obtained from MALDI-TOF analysis,[26] and, therefore, the MW values determined by GPC in our work were only used to reveal trends. ^{1}H NMR spectroscopy was also used to obtain molecular weights of ECP and PhCP initiated polymers by comparing the peak areas of the polymer isopropyl C-H signal at 3.9 ppm, with the ethoxy signal at 4.1 ppm (O-CH_2-) and the aromatic signal at 7.2-7.4 ppm arising from ECP and PhCP respectively. The MWs of CP and *i*-PrCP initiated polymers could not be determined by NMR due to the overlap of end group signals with those of the main chain. The M_n values determined by either GPC ($M_{n,GPC}$) or NMR ($M_{n,NMR}$) increased in proportion to the monomer:initiator (M:I) ratio (Table 1), and $M_{n,NMR}$ values were in good agreement with theoretical values.

As summarized in Table 1, polymerizations with all of the initiators gave moderate to high conversions for target degrees of polymerization (DPs) of 50, 100 and 200. Data for methyl 2-chloropropionate (MCP) initiated polymerizations described in Chapter 2 has been included for comparison. When DP = 200 was targeted, monomer

concentration was increased to 50% to speed up polymerization and promote monomer conversion. Polymerizations with target DP of 50 were used to study the kinetics of the ATRP. We observed almost no differences in the kinetic characteristics of these four polymerizations, showing that changing the substitution pattern on the propionyl fragment of the initiators did not affect the initiation and the propagation (Figure 2). Similar to our previous work on the ATRP of NIPAM using MCP initiator,[19] first-order kinetic plots showed slight curvature especially in the early stage of polymerization, which had been attributed to progressive catalyst deactivation rather than chain termination. The linear molecular weight ($M_{n,GPC}$) increase with conversion and the low PDIs (1.0–1.2) throughout the polymerization revealed good control in all the polymerizations. The apparent M_n values measured by GPC were about two to three times higher than expected, as reported by Müller's group.[26] (The MWs of these new PNIPAMs measured by GPC have all systematically appeared to be bigger than those made from the MCP initiator. It may be due to a deterioration of the GPC columns as in the intervening time, as a sample originally prepared using MCP now also showed an analogously higher MW.)

Therefore, 2-propanol has proven to be an effective solvent for the ATRP of NIPAM, suitable for a range of initiators, giving good conversion, controlled MW, and low PDI.

Table 1. Monomer Conversion, Molar Mass (M_n), and Polydispersity (M_w/M_n) Data for Atom Transfer Radical Polymerization (ATRP) of *N*-Isopropylacrylamide (NIPAM) in 2-propanol with Different Initiators[a]

initiator	$[M]_0:[I]_0$ (M/solvent) (w/w)	time (h)	conv (%)	$M_{n,th}$[b]	$M_{n,GPC}$[c]	$M_{n,NMR}$[d]	M_w/M_n[c]
CP	50:1 (1/2)	4.5	80	4500	11400		1.07
	100:1 (1/2)	7.6	78	8800	19100		1.08
	200:1 (1/1)	5.1	72	16300	57000		1.09
i-PrCP	50:1 (1/2)	4.5	87	4900	11100		1.11
	100:1 (1/2)	7.2	78	8800	20500		1.14
	200:1 (1/1)	5	85	19200	58400		1.12
ECP	50:1 (1/2)	4.5	81	4600	9700	4300	1.06
	100:1 (1/2)	7	79	8900	21000	7300	1.10
	200:1 (1/1)	5	79	17900	45100	15200	1.13
PhCP	50:1 (1/2)	4.5	82	4600	12500	4800	1.08
	100:1 (1/2)	7.6	85	9600	25000	9300	1.11
	200:1 (1/1)	5.1	81	18300	49900	18100	1.12
MCP	50:1 (1/2)	4	89	5 000	8 000	5 000	1.15
	100:1 (1/2)	7	91	10 300	17 300	8 400	1.13
	200:1 (1/1)	4.5	78	17 600	44 200	16 400	1.14

[a]Experimental conditions: typically 2 g of NIPAM; Initiator:CuCl:Me_6TREN = 1:1:1; room temperature. [b]$M_{n,th} = M_{NIPAM}[NIPAM]_0 conv/[MCP]_0$. [c]From GPC in 0.25% (w/v) Bu_4NBr/THF. [d]From ^1H NMR spectroscopy (500 MHz) in D_2O, 25 °C.

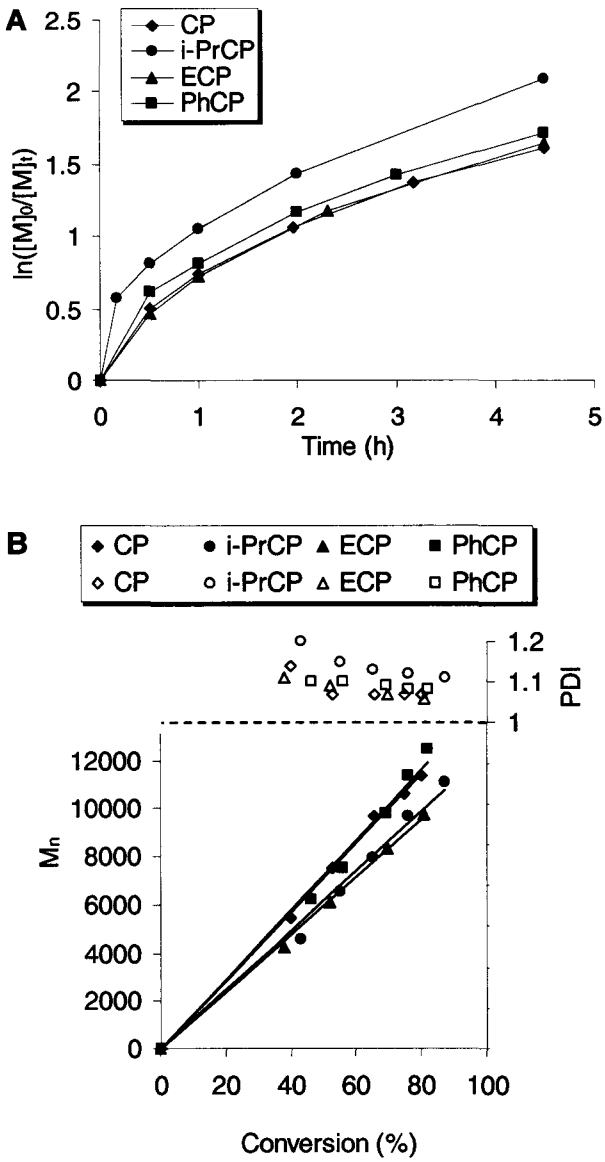

Figure 2. (A) Kinetic plot for the ATRP of NIPAM in *i*-PrOH with different initiators. (B) Dependence of molecular weight ($M_{n,GPC}$) and polydispersity (M_w/M_n) on conversion. Conditions: NIPAM/*i*-PrOH = 1/2 (w/w); NIPAM:initiator:CuCl:Me_6TREN = 50:1:1:1; room temperature. The lines in (A) serve as guides for the eye while those in (B) are best-fit lines.

3.2.2 Thermal Phase Transitions by Turbidimetry. Four PNIPAM samples of each end group type were prepared to study their thermal phase transitions with $M_{n,th}$ ranging from ~3 kDa to ~20 kDa. Each sample was designed to have MW similar to those of their counterparts in other end group types, so that the end group effect could be studied independent of the MW.

Cloud points of 1 wt % aqueous solutions of these PNIPAMs were measured by turbidimetry. Transmittance of the solution was recorded with increasing temperature. A slow heating rate of 0.2 °C/min was used in all the measurements to minimize the thermal lag between the sample cell and the solution. The cloud point of each sample was determined as the average of at least two independent scans.

Table 2 summarizes turbidimetry results and Figure 3 shows the transmittance vs. temperature plots (cloud point curves) for all the PNIPAMs with four different end groups. The polymers are designated by attaching the initiator used, namely, as PNIPAM-CP, PNIPAM-*i*-PrCP, PNIPAM-ECP, and PNIPAM-PhCP. PNIPAM-CP polymers showed sharp transitions, while PNIPAM-ECP and -PhCP showed apparent early onsets in their cloud point curves similar to that previously observed for PNIPAM-MCP.[19] These early onsets are most significant for low MW PNIPAMs, and can start as much as 5°C below the main transition, as seen for the PNIPAM-PhCP, which bears the most hydrophobic end group. However, the oligomers of PNIPAM-ECP discussed below do not show any such early onset, indicating that these early onsets, as well as the widths of the cloud point curves, are likely not due to micellization of low molecular weight fractions, but rather to differences in the rates of aggregation of the different PNIPAMs, which is beyond the

scope of this study. To avoid interference from these effects, we use the 50% transmittance points (50%T) to determine the cloud point, and additionally provide the 90%T point to give an indication of the width of the transition.

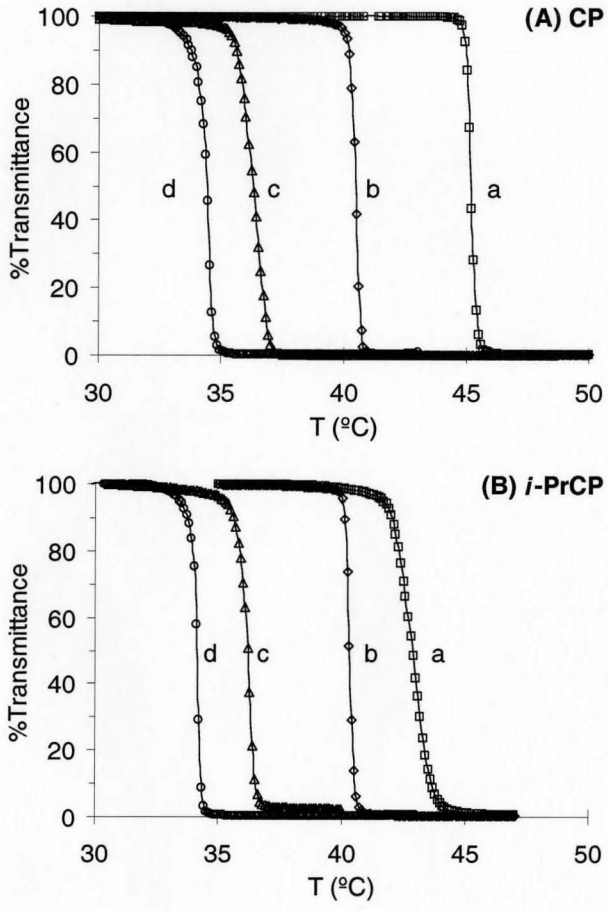

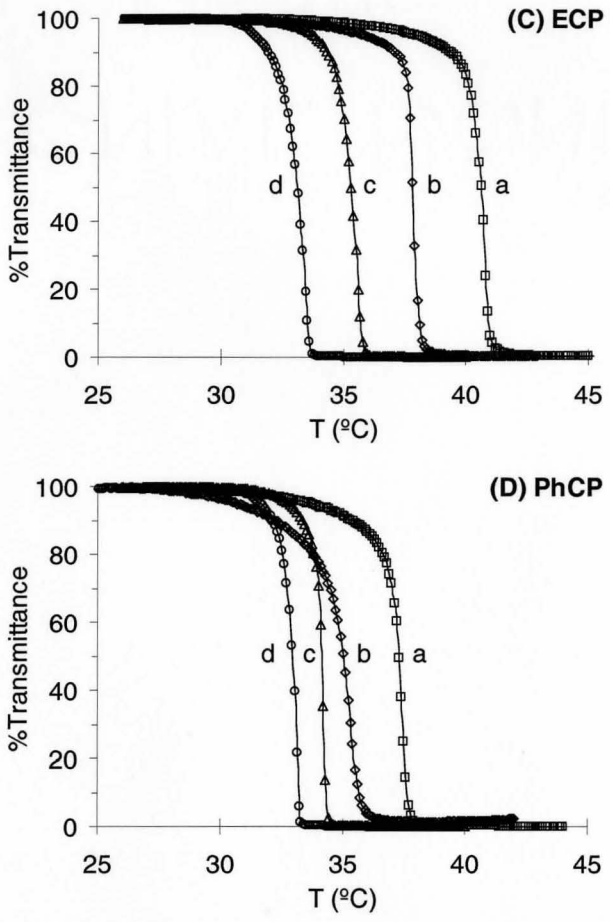

Figure 3. Transmittance vs. temperature for 1 wt % solutions of PNIPAM made by ATRP with the initiator of (A) CP: $M_{n,th}$ = a) 3.0, b) 4.5, c) 8.8, d) 16.3 kDa; (B) *i*-PrCP: $M_{n,th}$ = a) 3.1, b) 4.9, c) 8.8, d) 19.2 kDa; (C) ECP: $M_{n,th}$ = a) 2.9, b) 4.6, c) 8.9, d) 17.9 kDa; (D) PhCP: $M_{n,th}$ = a) 3.2, b) 4.6, c) 9.6, d) 18.3 kDa. Heating rate = 0.2 °C/min.

Table 2. Properties of Various PNIPAMs with Different Molar Mass (M_n) and End Groups in Aqueous Solution[a]

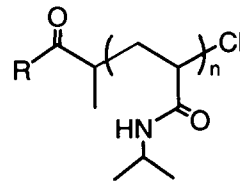

R	$M_{n,th}$ (Da)	$M_{n,GPC}$ (Da)	$M_{n,NMR}$ (Da)	PDI	phase transition temp (°C)		ΔH^c (kcal mol^{-1})
					Turbidity[b] (90/50%T)	HS-DSC[c] ($T_m/T_{1/2}$)	
-NH_2	3000	7500		1.07	44.9/45.3	48.4/6.8	1.04
	4500	11400		1.07	40.2/40.7	42.9/4.6	1.34
	8800	19100		1.08	35.6/36.3	39.0/2.8	1.39
	16300	57000		1.09	33.8/34.4	36.1/2.1	1.58
-NH-*i*-Pr	3100	6500		1.15	42.0/42.9	47.1/7.8	1.01
	4900	11100		1.11	40.1/40.3	42.2/4.3	1.24
	8800	20500		1.14	34.7/36.0	38.1/2.6	1.39
	19200	58400		1.12	33.7/34.1	35.4/2.0	1.61
-OEt	2900	6100	3000	1.09	39.3/40.6	42.2/6.2	1.33
	4600	9700	4300	1.06	37.1/37.8	39.7/3.4	1.33
	8900	21000	7300	1.10	33.9/35.2	37.0/2.6	1.46
	17900	45100	15200	1.13	31.9/33.3	35.0/1.9	1.62
-NHPh	3200	7500	3200	1.10	35.4/37.4	39.2/4.2	1.32
	4600	12500	4800	1.08	32.2/35.1	37.6/3.3	1.33
	9600	25000	9300	1.11	33.3/34.2	35.6/2.4	1.49
	18300	49900	18100	1.12	32.0/32.8	34.2/1.9	1.55
-OMe	3300	4600	2800	1.07	36.3/43.0		
	5000	8000	5000	1.15	37.5/38.9		
	8600	14300	6700	1.13	36.1/36.4		
	17600	35600	15700	1.13	34.4/34.6		

[a] Parameters defined in Table 1. [b] 1 wt % solution; heating rate = 0.2 °C/min. [c] 1 wt % solution; heating rate = 1.0 °C/min; values are kilocalories per mole of monomer

repeating units.

For each end group, the polymers showed inverse MW dependence of the cloud point (Figure 4). For instance, the cloud point (50%T) of PNIPAM-CP polymers dropped from 45.3 to 34.4 °C as the MW ($M_{n,th}$) increased from 3.0 to 16.3 kDa, while for PNIPAM-PhCP, the cloud point dropped from 37.4 to 32.8 °C as the MW ($M_{n,th}$) increased in a similar range from 3.2 to 18.3 kDa.

The end group effect was most significant for the low MW samples. PNIPAM-*i*-PrCP, designed to have the no initiator end group effect and hence represent an ideal PNIPAM, had a cloud point of 42.9 °C at 3 kDa MW. In comparison, the hydrophilic propionamide end group elevated the cloud point to 45.3 °C while the hydrophobic ethoxypropionate and phenylpropionamide end groups lowered the cloud point to 40.6 °C, and 37.4 °C, respectively. Thus, a 7.9 °C drop in cloud point was caused just by the addition of a phenyl group at the chain end. Similarly, changing the chain end from methyl (PNIPAM-MCP) to ethyl (PNIPAM-ECP) lowered the cloud point by 2.4 °C for the 3 kDa chains. PNIPAM-MCP had cloud points similar to those of PNIPAM-*i*-PrCP, indicating that the weakly hydrophobic methyl propionate end group does not have a significant effect on the cloud point, at least in the MW range studied.

The end group effect is much less remarkable for longer chains. For samples having MW around 16 to 18 kDa, the cloud point only decreased 1.6 °C from 34.4 °C for PNIPAM-CP to 32.8 °C for PNIPAM-PhCP. Clearly, the MW dependence of the cloud point is a combination of the end group effect and the MW effect. Hydrophilic end groups exacerbate the MW effect, while hydrophobic end groups can mitigate the MW

dependence or perhaps reverse it if the end group were hydrophobic enough. PNIPAM-PhCP gave the smallest MW dependence among the four series studied here. However, in the range of MWs and end groups studied, the MW effect still dominates, such that all the chains show inverse MW dependence. PNIPAM-*i*-PrCP polymers are considered to have no end group effect except the chlorine at the terminating end, so these polymers most closely reflect the authentic MW effect.

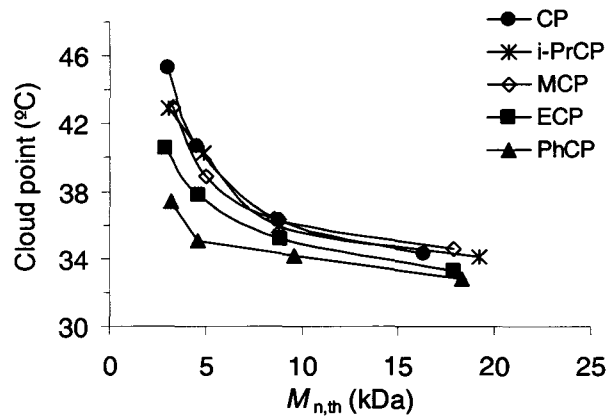

Figure 4. Cloud point (50%T) vs. polymer molecular weight ($M_{n,th}$) for narrow-disperse PNIPAM samples with different end groups made by ATRP. Cloud points determined by turbidimetry on 1 wt % solutions, heating rate = 0.2 °C/min.

3.2.3 NIPAM Oligomers. Two oligoNIPAM samples with degrees of oligomerization of 10 (oligoNIPAM-10, $M_{n,GPC}$ = 2530, $M_{n,NMR}$ = 1070, PDI = 1.20) and 4 (oligoNIPAM-4, $M_{n,NMR}$ = 460, GPC was unable to determine the M_n and PDI as the MW of this oligomer exceeded the MW range of GPC standard samples) were prepared with the ECP initiator to test our hypothesis that, for very low MW oligomers, the end group

effect may dominate and thus they may have lower LCST instead. Their GPC traces are shown in Figure 5 A. The bimodal MW distribution of oligoNIPAM-4 might be due to the improved GPC resolution at the low MW end, which enables resolution of individual oligomers with different DP, or the termination from high radical concentration at the initiation. However, turbidimetry showed that oligoNIPAM-10 has a cloud point of 50.9 °C and oligoNIPAM-4 has a cloud point of 70.4 °C. OligoNIPAM-10 still has a sharp transition, but oligoNIPAM-4 has a very broad transition in transmittance over 10 °C (Figure 5 B). Transmittance stopped decreasing at about 10% and began to increase in both cases, which indicates aggregation and/or settling of sample, resulting in less light being scattered. This is commonly seen for all the samples, but it happens faster for these oligomers.

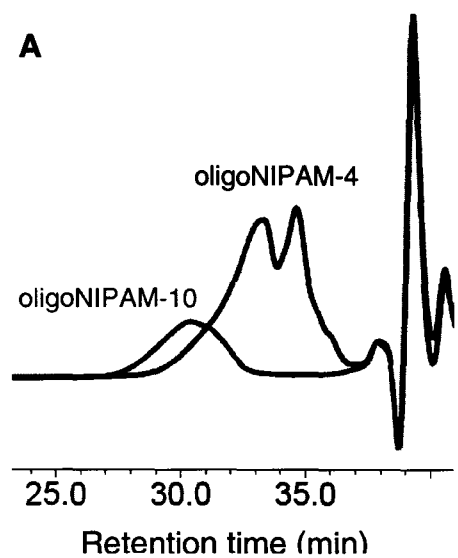

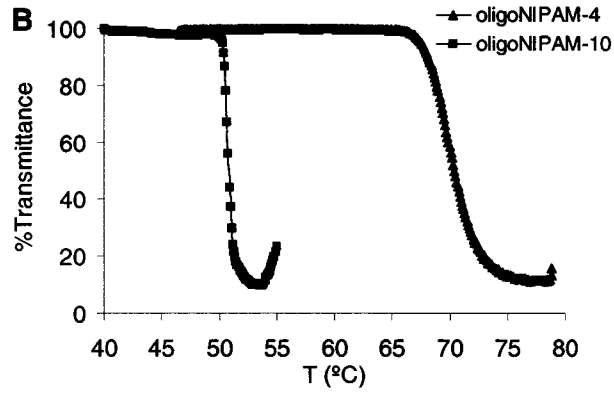

Figure 5. NIPAM oligomers initiated with ECP. (A) GPC traces; (B) Cloud point curves (transmittance vs. temperature) for 1 wt % solutions.

3.2.4 High-sensitivity Differential Scanning Calorimetry (Microcalorimetry).

High-sensitivity differential calorimetry (HS-DSC) was also used to investigate the phase transition of these polymer solutions. HS-DSC records the changes of partial excess heat capacity C_p of the solutions as a function of temperature. It has been widely used to study the "coil-to-globule" transition of PNIPAM[1,12,16,27,30] and other thermoresponsive polymers[3,5,7,12,16,28] and their hydrogels,[29] and to provide information about the temperature and enthalpy change of the phase transition. It has been widely claimed that varying the scanning rate over a wide range has little or no effect on the shape of the thermograms or the transition temperature.[1,7,12,16,27-29] For example, Winnik et al[7,28] (10-90 °C/h) and Mikheeva et al[29] (15-120 °C/h) found no effect, while Zhu et al[3] observed only a slight upward shift of transition temperature when the scanning rate was increased 10-fold. However, it has been recently reported that the phase transition temperature increased linearly with the heating rate, which was attributed to more intrachain

contraction and less interchain association in a fast heating scan.[30] The reproducibility of the results was demonstrated in these previous studies by repeated heating scans at the same heating rate. Therefore it is commonly concluded that the heat transfer in microcalorimetry is so effective that the characteristic times of the transitions of polymers are shorter than those of the thermal equilibration of the cells.

To verify that our calorimetric measurements are independent of the heating rate and therefore are thermodynamic parameters, we first studied the heating rate dependence and reproducibility of the thermograms. 1 wt % aqueous PNIPAM solutions were held in a 0.5121 ml DSC cell and scanned sequentially with heating rates of 15, 30, and 60 °C/h. Before each heating scan, the sample was held at 10 °C for 10 min. All samples were cooled at 90 °C/h unless indicated and only heating scans were considered.

We observed that changing the heating rate from 15 to 60 °C/h did not affect the peak temperature, T_m, but only slightly broadened the peak for the polydisperse PNIPAM made by AIBN. However, for PNIPAM made by ATRP, slow heating rates or holding the sample above the LCST resulted in the formation of an extra peak at the low-temperature side of the original transition in subsequent scans. Low MW samples were found more vulnerable to this change than high MW ones (For more information, see the appendix A). We suspected that, in the collapsed state, PNIPAMs made by ATRP may not be colloidally stable and may aggregate and settle to cause the extra peak in a subsequent DSC run of the same sample.

Particular care is hence required to perform microcalorimetry on such PNIPAM solutions. To avoid the formation of the extra peak, we only used the result from the first

heating scan of every sample and a heating rate of 60 °C/h for our measurements. The endotherm maximum, onset and width were not significantly altered when slower scan rates (15, 30 °C/h) were used. Reproducibility of the results was checked by repeating measurements with freshly prepared sample solution. The DSC results are shown in Table 2 and Figure 6 shows the microcalorimetric endotherms for each family of PNIPAMs.

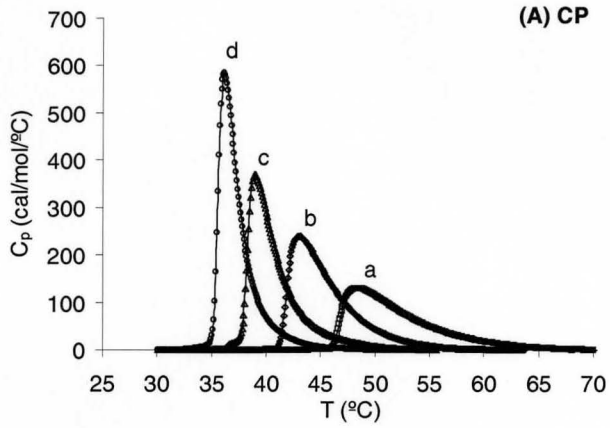
(A) CP
700
600
500
400
300
200
100
0
C_p (cal/mol/ºC)
d
c
b
a
25 30 35 40 45 50 55 60 65 70
T (ºC)

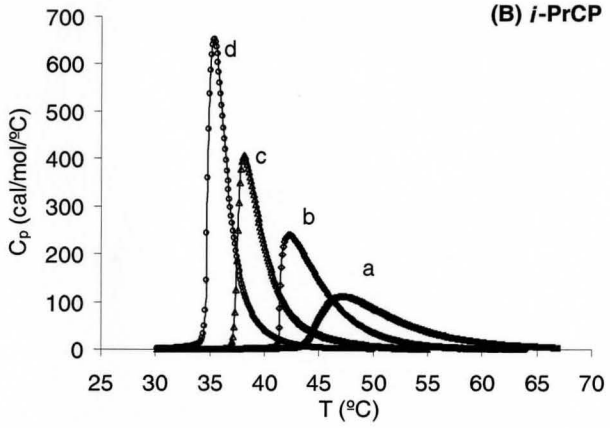
(B) *i*-PrCP
700
600
500
400
300
200
100
0
C_p (cal/mol/ºC)
d
c
b
a
25 30 35 40 45 50 55 60 65 70
T (ºC)

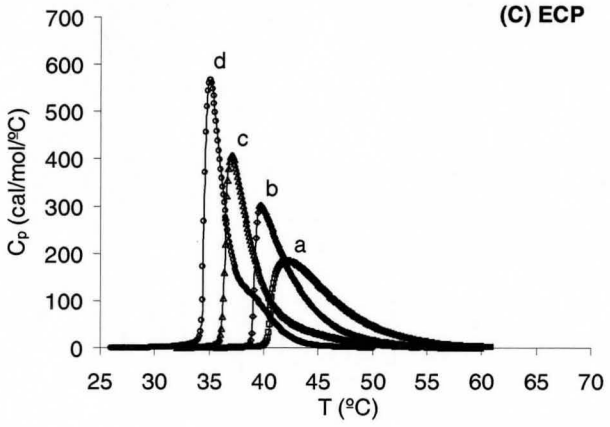
(C) ECP
700
600
500
400
300
200
100
0
C_p (cal/mol/ºC)
d
c
b
a
25 30 35 40 45 50 55 60 65 70
T (ºC)

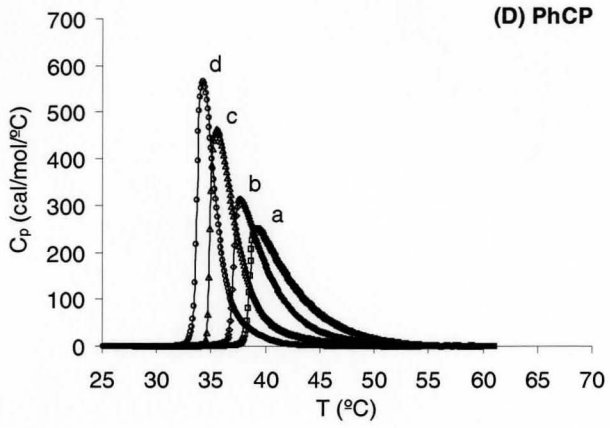

Figure 6. Microcalorimetric endotherms of 1 wt % aqueous solutions of (A) PNIPAM-CP, $M_{n,th}$ = a) 3.0, b) 4.5, c) 8.8, d) 16.3 kDa; (B) PNIPAM-*i*-PrCP, $M_{n,th}$ = a) 3.1, b) 4.9, c) 8.8, d) 19.2 kDa; (C) PNIPAM-ECP, $M_{n,th}$ = a) 2.9, b) 4.6, c) 8.9, d) 17.9 kDa; (D) PNIPAM-PhCP, $M_{n,th}$ = a) 3.2, b) 4.6, c) 9.6, d) 18.3 kDa. Heating rate = 60 °C/h.

Microcalorimetry results showed the same tendency of MW effect and end group effect as revealed by turbidimetry. Hydrophobic end groups decreased the transition temperature while the hydrophilic amide end group increased the transition temperature. All PNIPAMs in our study had inverse MW dependence. The peak temperature, T_m, from microcalorimetry of each sample was 2-3 °C higher than its cloud point measured by turbidimetry. DSC peaks broadened from about 2 °C in the peak width at half height, $T_{1/2}$, for the longest chain to 4-7 °C for the shortest, despite similar PDI values. This is not surprising as in the low MW range the phase transition temperature is more sensitive to MW changes, so residual polydispersities play a more important role.

While in the cloud point curves measured by turbidimetry, PNIPAM–CP and PNIPAM–*i*–PrCP had sharper transitions than the PNIPAMs with hydrophobic end

groups, the DSC studies showed PNIPAM-CPs to have the broadest phase transitions. The polar CP end group further increases the phase transition temperature, especially for the low MW fractions. In cloud point measurements, this effect can be masked by the dominant high MW fractions that phase separate first. In HS-DSC, the phase separation of these low MW fractions is detected and results in a broader distribution after T_m in the thermogram. Hence, a sharper transition in the cloud point curve does not necessarily indicate a narrower real thermal phase transition.

The enthalpy of phase transition (ΔH) exhibited a slight direct MW dependence regardless of end group down to $M_{n,th}$ ~ 5 kDa. ΔH decreased from 1.6 kcal mol^{-1} for the longest samples ($M_{n,th}$ ~ 18 kDa) to 1.3 kcal mol^{-1} for the second shortest ($M_{n,th}$ ~ 5 kDa). Interestingly, when the MW further decreased from 5 to 3 kDa, for PNIPAM with hydrophobic end groups, PNIPAM-ECP and PNIPAM-PhCP, ΔH remained constant about 1.3 kcal mol^{-1}. In contrast, PNIPAM with hydrophilic end groups, PNIPAM-*i*-PrCP and PNIPAM-CP, showed a sudden decrease in ΔH from 1.3 to 1.0 kcal mol^{-1} (Figure 7). This difference may reflect the end group effect on the thermal phase transition. Hydrophobic end groups may help the desolvation of the polymers above the cloud point, while hydrophilic end groups may interfere with it. For example, the low MW fraction of PNIPAM-CP (M_n ~ 3 kDa) may not undergo phase transition during heating leading to a 20% lower apparent ΔH. This effect may only manifest in very low MW samples, where the end groups are present in larger molar proportion to the polymer chain.

The ΔH values we obtained are within the range, 0.8-1.9 kcal mol^{-1}, reported for linear PNIPAM.[1,7,11,12,18,27,28,30] Winnik et al reported a strong direct dependence of ΔH on

MW for narrow-disperse thermoresponsive poly(2-isopropyl-2-oxazoline)[28] and Zhu et al discovered a significant inverse dependence of ΔH on MW over a much wider MW range for thermoresponsive poly(*N,N*-diethylacrylamide),[3] while other reports do not seem to present a clear MW dependence.[1,7,11,12]

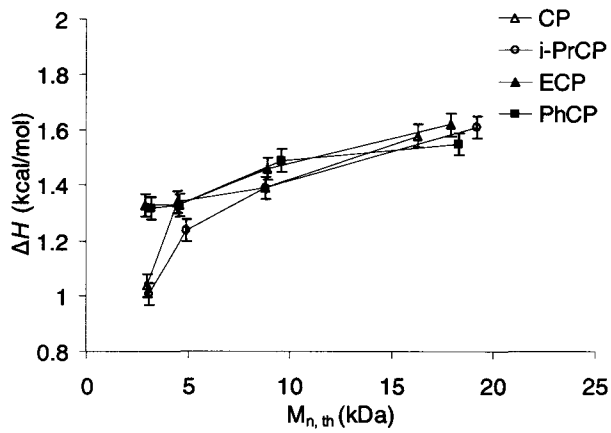

Figure 7. Plots of the enthalpy of transition as a function of molecular weight of 1 wt % aqueous solution of the PNIPAM made by ATRP with different initiators. Heating rate = 60 °C/h.

3.2.5 Effect of Polymer Concentration. The concentration dependence of the phase transition was studied using two samples, one made by ATRP (PNIPAM-*i*-PrCP, $M_{n,th}$ = 19.2 kDa) and the other made with AIBN, varying their concentrations from 0.10 to 8.0%. They both showed the same trend: as the concentration increases, their cloud points decrease (Figure 8), demonstrated by turbidimetry for both (Figure 9) and HS-DSC for PNIPAM-*i*-PrCP (Figure 10). The concentration dependence is stronger in the dilute range below 1 wt %. The cloud point curves showed that more concentrated samples tend

to aggregate and settle more easily, which resulted in an increase in transmittance after the initial decrease. In addition, the samples made by ATRP tend to settle more readily than the one made by AIBN (Figure 9). This supports our hypothesis that the change in the DSC thermogram of samples made by ATRP may be caused by the more efficient aggregation and settling of PNIPAM globules above the LCST.

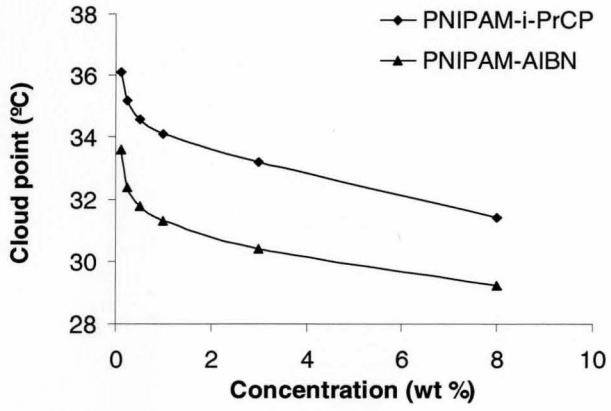

Figure 8. Effect of polymer concentration on the phase separation temperature of aqueous solutions of PNIPAM-*i*-PrCP ($M_{n,th}$ = 19.2 kDa) and PNIPAM-AIBN ($M_{n,GPC}$ = 28.9 kDa) as measured by turbidimetry.

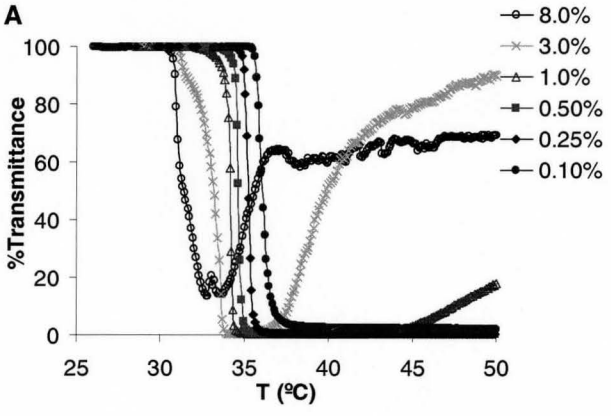

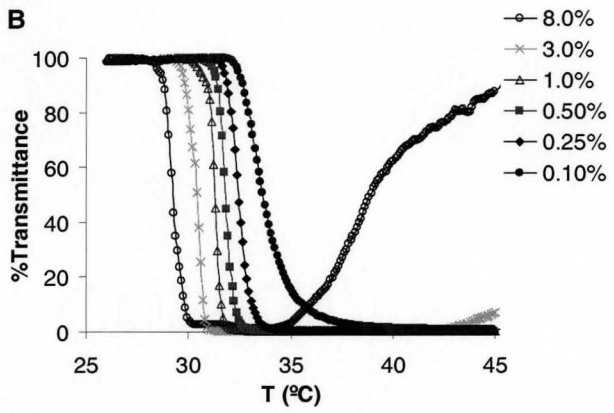

Figure 9. Transmittance vs. temperature for aqueous solutions of (A) PNIPAM-*i*-PrCP ($M_{n,th}$ = 19.2 kDa); (B) PNIPAM-AIBN ($M_{n,GPC}$ = 28.9 kDa) with different concentrations.

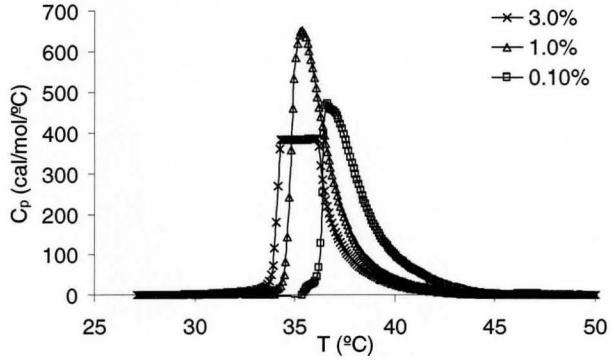

Figure 10. Microcalorimetric endotherms of aqueous solutions of PNIPAM--*i*-PrCP ($M_{n,th}$ = 19.2 kDa) with different concentrations. (Note: the 3.0 % PNIPAM sample exceeded the detection limit of the HS-DSC, and goes off-scale.)

PNIPAM made with persulfate initiator has been found to be able to form a stable colloidal suspension upon heating[31,32] where the charged sulfate end group provides colloidal stability. PNIPAM and another thermoresponsive polymer, poly(*N*-

vinylcaprolactam) (PVCL), prepared with neutral initiator AIBN were also observed by light scattering (LS) to give aggregates with constant hydrodynamic radius when held above their LCST, for days.[7,33] It was also found that low MW samples lead to larger aggregate size. It was believed that partially solvated chains on surfaces of the aggregates provided steric stabilization against further aggregation. Besides, the polymer solutions in these LS studies are at least 10-fold more diluted than the concentration we use and thus flocculation is more unfavorable. Our low MW, narrow-disperse PNIPAM samples were observed to be colloidally less stable than the polydisperse PNIPAM-AIBN, which possesses a much larger high MW fraction. We suspect that when the PNIPAM chains are too short, they are poor steric stabilizers for the aggregate. The aggregates keep growing until a certain size where the aggregates are no longer colloidally stable and they settle, especially under the relatively high concentrations used for turbidimetry and HS-DSC. The aggregation behaviors of high and low MW PNIPAMs will be subject to further investigation by light scattering.

3.3 Conclusion

We have successfully prepared four series of narrow-disperse PNIPAM (five including the MCP-initiated polymers discussed in Chapter 2) with end groups of varying polarity by ATRP using corresponding chloropropionate and chloropropionamide initiators. Improved control over MW and end group enabled us to resolve the MW and end group effects.

Both turbidimetry and microcalorimetry were used to investigate the thermal phase transition of aqueous solutions of these PNIPAMs. Both methods showed reasonable agreement, but care was needed to obtain reproducible microcalorimetric results. As expected, hydrophilic end groups increased the LCST of the polymers, while hydrophobic end groups decreased it. This effect is most significant for the shortest chains, where it results in an 8 °C difference in LCST upon going from amide to phenylamide. The end group effect diminishes rapidly when MW is above 10 kDa. The LCST of PNIPAM was observed to decrease with increasing MW for all the four series of samples as was observed with the MCP-initiated PNIPAM. Therefore in the range of MW and end groups studied, the MW effect dominates over the end group effect on LCST. Homogeneous PNIPAM samples bearing an end group that is identical to the repeating unit give similar LCST values with those from methoxypropionate terminated PNIPAMs in our previous report.[19]

The enthalpy of transition was found to decrease slightly with decreasing MW. But when the lowest MW is approaching, hydrophobic end groups hold the ΔH constant, while the hydrophilic end groups further decrease the ΔH.

References

(1) Schild, H. G.; Tirrell, D. A. *J. Phys. Chem.* **1990**, *94*, 4352-4356.

(2) Aoshima, S.; Oda, H.; Kobayashi, E *J. Polym. Sci. A: Polym. Chem.* **1992**, *30*, 2407-2413.

(3) Lessard, D. G.; Ousalem, M.; Zhu, X. X. *Can. J. Chem.* **2001**, *79*, 1870-1874.

(4) Bütün, V.; Armes, S. P.; Billingham, N. C. *Polymer* **2001**, *42*, 5993-6008.

(5) Kunugi, S.; Tada, T.; Tanaka, N.; Yamamoto, K.; Akashi, M. *Polym. J.* **2002**, *34*, 383-388.

(6) Xue, W.; Huglin, M.B.; Jones, T.G.J. *Macromol. Chem. Phys.* **2003**, *204*, 1956-1965.

(7) Laukkanen, A.; Valtola, L.; Winnik, F. M.; Tenhu, H. *Macromolecules* **2004**, *37*, 2268-2274.

(8) Tong, Z.; Zeng, F.; Zheng, X. *Macromolecules* **1999**, *32*, 4488-4490; Zheng, X.; Tong, Z.; Xie, X.; Zeng, F. *Polym. J.* **1998**, *30*, 284-288.

(9) Liu, Q.; Yu, Z.; Ni, P. *Colloid Polym. Sci.* **2004**, *282*, 387-393.

(10) Fujishige, S.; Kubota, K.; Ando, I. *J. Phys. Chem.* **1989**, *93*, 3311-3313.

(11) Otake, K.; Inomata, H.; Konno, M.; Saito, S. *Macromolecules* **1990**, *23*, 283-289.

(12) Tiktopulo, E. I.; Uversky, V. N.; Lushchik, V. B.; Klenin, S. I.; Bychkova, V. E.; Ptitsyn, O. B. *Macromolecules* **1995**, *28*, 7519-7524.

(13) Chung, J. E.; Yokoyama, M.; Aoyagi, T.; Sakurai, Y.; Okano, T. *J. Controlled Release* **1998**, *53*, 119-130.

(14) Chung, J. E.; Yokoyama, M.; Suzuki, K.; Aoyagi, T.; Sakurai, Y.; Okano, T. *Colloids Surf. B: Biointerfaces* **1997**, *9*, 37-48.

(15) Yamazaki, A.; Song, J. M.; Winnik, F. M.; Brash, J. L. *Macromolecules* **1998**, *31*, 109-115.

(16) Baltes, T.; Garret-Flaudy, F.; Freitag, R. *J. Polym. Sci. A: Polym. Chem.* **1999**, *37*, 2977-2989.

(17) Ringsdorf, H.; Venzmer, J.; Winnik, F. M. *Macromolecules* **1991**, *24*, 1678-1686.

(18) Kujawa, P.; Winnik, F. M. *Macromolecules* **2001**, *34*, 4130-4135.

(19) Xia, Y.; Yin, X.; Burke, N. A. D.; Stover, H. D. H. *Macromolecules* **2005**, *38*, 5937-5943.

(20) Ciampolini, M.; Nardi, N. *Inorg. Chem.* **1966**, *5*, 41-44.

(21) Rademacher, J. T.; Baum, M.; Pallack, M. E.; Brittain, W. J.; Simonsick, W. J. *Macromolecules* **2000**, *33*, 284-288.

(22) Teodorescu, M.; Matyjaszewski, K. *Macromolecules* **1999**, *32*, 4826-4831.

(23) Teodorescu, M.; Matyjaszewski, K. *Macromol. Rapid Commun.* **2000**, *21*, 190-194.

(24) Neugebauer, D.; Matyjaszewski, K. *Macromolecules* **2003**, *36*, 2598-2603.

(25) Yin, X.; Stöver, H. D. H. *Macromolecules*, **2005**, *38*, 2109-2115.

(26) Schilli, C.; Lanzendörfer, M. G.; Müller, A. H. E. *Macromolecules* **2002**, *35*, 6819-6827.

(27) Tiktopulo, E. I.; Bychkova, V. E.; Rička, J.; Ptitsyn, O. B. *Macromolecules* **1994**, *27*, 2879-2882.

(28) Diab, C.; Akiyama, Y.; Kataoka, K.; Winnik, F. M. *Macromolecules* **2004**, *37*, 2556-2562.

(29) Mikheeva, L. M.; Grinberg, N. V.; Mashkevich, A. Y.; Grinberg, V. Y.; Thanh, L. T. M.; Makhaeva, E. E.; Khokhlov, A. R. *Macromolecules* **1997**, *30*, 2693-2699.

(30) Ding, Y.; Ye, X.; Zhang, G. *Macromolecules* **2005**, *38*, 904-908.

(31) Chan, K.; Pelton, R.; Zhang, J. *Langmuir* **1999**, *15*, 4018-4020.

(32) Gorelov, A. V.; Du Chesne, A.; Dawson, K. A. *Physica A* **1997**, *240*, 443-452.

(33) Li, M.; Wu, C. *Macromolecules* **1999**, *32*, 4311-4316.

Appendix A. Optimizing HS-DSC Conditions

Initial experiments used a 1 wt % aqueous solution of PNIPAM prepared previously by conventional radical polymerization using AIBN ($M_{n,GPC}$ = 28.9 kDa, PDI = 2.0).[1] This sample was scanned from 10 to 50 °C at 15, 30, and 60 °C/h sequentially, yielding asymmetrical peaks with a relatively sharp onset of the peak and a more gradual decrease after the maximum as typically seen in the literature, and a peak temperature, T_m = 33.1 °C (Figure 1). Increasing the scanning rate did not affect T_m, but the peak broadened very slightly with subsequent scans giving a 0.2 °C increase in the peak width at half height, $T_{1/2}$, and an increase in the enthalpy change of transition, ΔH, from 1.36 to 1.42 cal mol^{-1}.

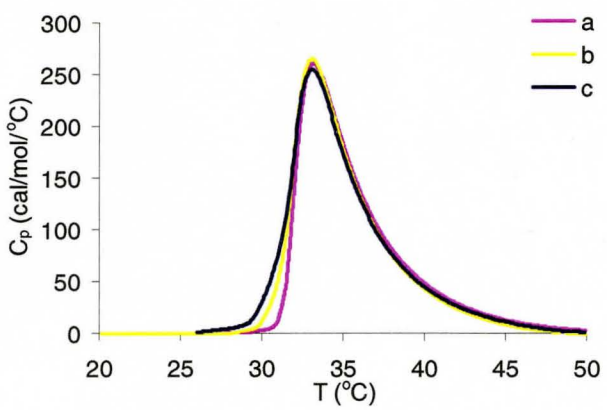

Figure 1. Microcalorimetric endotherms of three successive scans on a 1 wt % aqueous solution of PNIPAM sample prepared using AIBN ($M_{n,GPC}$ = 28.9 kDa, PDI = 2.0)[22]. Heating rate = (a) 15 °C/h; (b) 30 °C/h; (c) 60 °C/h.

Surprisingly, a much more complicated situation exists for the narrow-disperse PNIPAMs prepared by ATRP. PNIPAM-PhCP ($M_{n,th}$ = 18.3 kDa) was scanned repeatedly at 60 °C/h, and gave a reproducible sharp and asymmetrical peak with T_m = 34.2 °C and $T_{1/2}$ = 1.9 °C (Figure 2 A). When different heating rates were used for a newly prepared solution of the same sample, the first heating scan at 15 °C/h gave a similar but slightly narrower peak ($T_{1/2}$ = 1.7 °C), which overlapped well with the peaks obtained at 60 °C/h. However, the peak split and significantly broadened in subsequent scans at 30 and 60 °C/h, and a new peak around 33 °C appeared. This is clearly caused by incomplete re-solvation of the collapsed chains prior to the next heating scan. Subsequently the sample was held at 10 °C for 10 h, which should facilitate the re-solvation, and then scanned again at 60 °C/h. Interestingly, the new peak partially vanished and the thermogram was closer to the original shape, although the peak was broader with a shift of 0.5 °C lower on the onset temperature (Figure 2 B). It is worth noting that this recovery is slow as a sample held at 10 °C for only 2 h showed no apparent change. The same behavior was observed from samples made with other initiators, for example PNIPAM-ECP ($M_{n,th}$ = 17.9 kDa) (Figure 3), so this behavior is not caused by one specific end group.

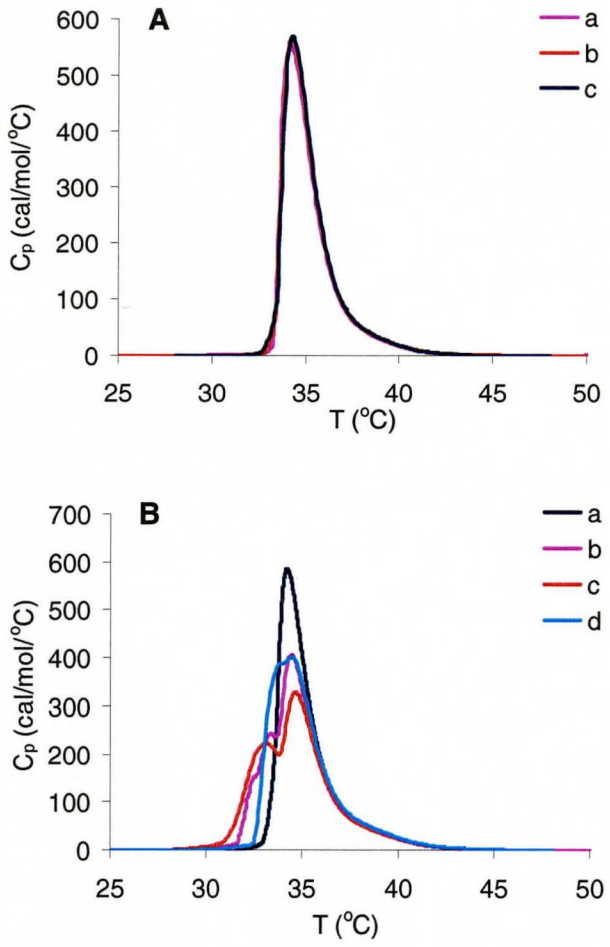

Figure 2. Microcalorimetric endotherms of 1 wt % aqueous solution of PNIPAM-PhCP ($M_{n,th}$ = 18.3 kDa). (A) Successive scans with heating rate = (a), (b), and (c) 60 °C/h. (B) Successive scans with heating rate = (a) 15 °C/h; (b) 30 °C/h; (c) 60 °C/h; (d) 60 °C/h after holding at 10 °C for 10h.

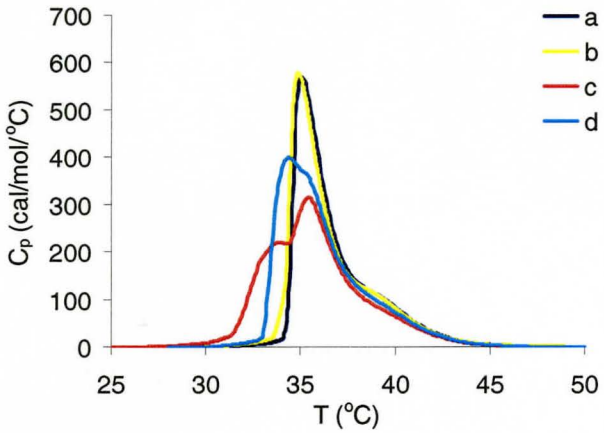

Figure 3. Microcalorimetric endotherms of four successive scans of a 1 wt % aqueous solution of PNIPAM-ECP ($M_{n,th}$ = 17.9 kDa). Heating rate = (a) 60 °C/h; (b) 15 °C/h; (c) 60 °C/h; (d) 60 °C/h after holding at 10 °C for 9h.

To further probe this question, a sample with a lower MW (PNIPAM-PhCP, $M_{n,th}$ = 9.6 kDa) was first scanned twice at 60 °C/h, after which T_m and $T_{1/2}$ did not change, although a small shoulder on the low-temperature side was seen. The sample was then held at 60 °C for 3 h. The following scan at 60 °C revealed the similar extra peak at lower temperature (Figure 4). Therefore, this confirms that the new peak is not due to a slow heating rate but rather to the long time above LCST where the chains desolvate to collapse into globular structure, aggregate, and settle.

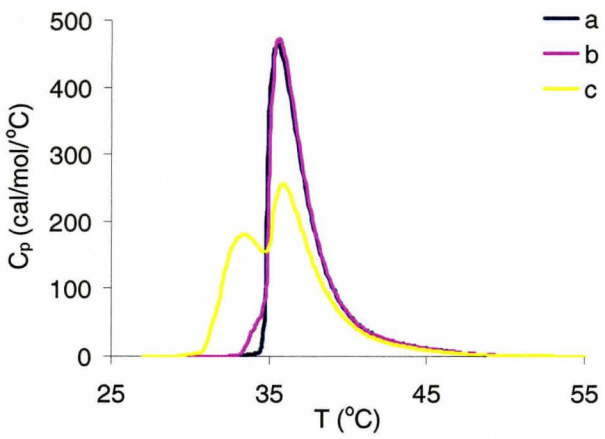

Figure 4. Microcalorimetric endotherms for three successive scans of a 1 wt % aqueous solution of PNIPAM-PhCP ($M_{n,th}$ = 9.6 kDa). Heating rate = (a) 60 °C/h; (b) 60 °C/h; (c) 60 °C/h after held at 60 °C for 3h.

We further found that samples with smaller MW are more vulnerable to this change. When the MW is less than 5 kDa, the extra peak on the low-temperature side is seen during the second heating scan, even if the first scan used a rate of 60 °C/h (Figure 5).

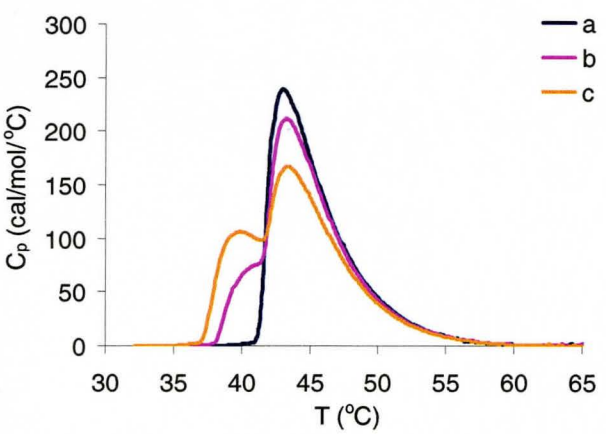

Figure 5. Microcalorimetric endotherms of three successive scans of a 1 wt % aqueous solution of PNIPAM-CP ($M_{n,th}$ = 4.5 kDa). Heating rate = (a), (b), (c) 60 °C/h.

A slow cooling rate, 20 °C/h, made the endotherm completely shift to low temperature with a broad shoulder on the high-temperature side (Figure 6), confirming that extended time at temperatures above LCST during one heating-and-cooling cycle, 10-80 °C, facilitated the formation of the new peak.

After scan c in Figure 6, the solution was cooled to 10 °C and then removed from the cell with a syringe. The cell was then washed with methanol and distilled water to remove residual PNIPAM solution, after which a blank scan with pure water injected into the sample cell showed only a flat baseline. Therefore there is no irreversible binding of the polymer chains to the cell wall to cause the extra peak. The same sample solution was then injected back to the sample cell and scanned three times with a heating rate of 60 °C/h and a cooling rate of 90 °C/h. Interestingly, the entire low-temperature side of the peak (scan d in Figure 6) including the onset temperature and the peak temperature shifted 2 °C higher than the curve from the first heating scan (scan a in Figure 6) while the high-temperature side of the peak still overlapped with the first scanning curve. This also resulted in a decrease in the enthalpy change from 1.33 kcal mol^{-1} for scan a to 0.97 kcal mol^{-1} for scan d, indicating a loss of 25% of the polymer. Further heating still developed an extra peak at lower temperature. Considering the high accuracy of microcalorimetry, the enthalpy decrease shows that part of the material was not fully solvated back into the solution when the first three heating-and-cooling cycles were

finished and the sample was cooled to 10 °C, and therefore this portion of sample was left in the cell and washed out during cleaning. This portion of sample may possess a higher MW which displays a lower LCST, so when the remaining sample was scanned, it gave a higher transition temperature. This is reminiscent of thermal fractionation where high MW fractions are more difficult to solvate and can be separated from low MW fractions. To test this hypothesis, a very careful and accurate comparison of the MW and PDI of the original sample and the final sample by MALDI-TOF is required.

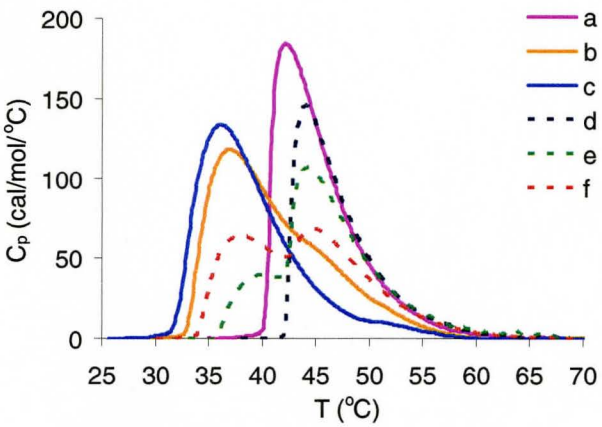

Figure 6. Microcalorimetric endotherms of 1 wt % aqueous solution of PNIPAM-ECP ($M_{n,th}$ = 2.9 kDa). First three cycles, 10-80 °C, are in solid line; (a), (b), (c) heating rate = 60 °C/h, cooling rate = 20 °C/h. Second three cycles, 10-80 °C, after sample removal, cell cleaning and reintroduction of the sample, are in dashed line; (d), (e), (f) heating rate = 60 °C/h, cooling rate = 90 °C/h.

A PNIPAM-*i*-PrCP ($M_{n,th}$ = 19.2 kDa) solution at a much lower concentration, 0.10 wt %, was also scanned at different heating rates. In contrast to 1.0 wt % solutions

used above, all the resultant thermograms overlapped when the heating rate was increased from 15 to 30 to 60 °C/h sequentially (Figure 7). This supports the idea that aggregation, settling, and poor re-dissolution of PNIPAM may be responsible for the extra peak in the thermograms. In the more diluted solution, PNIPAM globules may form stable suspensions rather than aggregate, so reproducible thermograms were obtained at different heating rates.

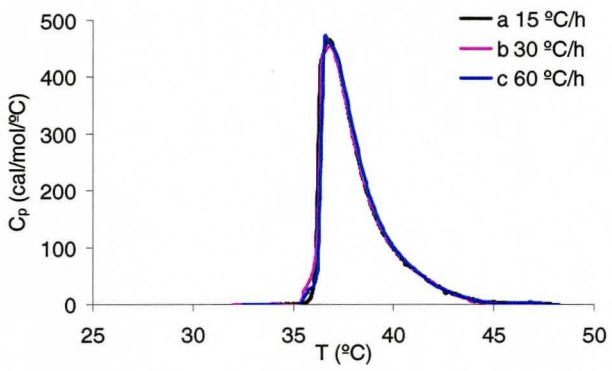

Figure 7. Microcalorimetric endotherms of three successive scans on a 0.1 wt % aqueous solution of PNIPAM-*i*-PrCP ($M_{n,th}$ = 19.2 kDa). Heating rate = (a) 15 °C/h; (b) 30 °C/h; (c) 60 °C/h.

In summary, we attribute the formation of the extra peak in HS-DSC scans to sedimentation followed by very slow re-homogenization by diffusion. Thermally induced phase separation of aqueous polymer solutions has been proposed to take place in two stages. Individual polymer chains first desolvate and form primary aggregates, which may then macroscopically aggregate.[2-4] At higher concentrations, further aggregation may lead to sedimentation. After the solution is cooled below its LCST, however, without stirring the settled aggregates can be very difficult to re-dissolve. While they rehydrate upon

decreasing the temperature below the cloud point, the sample solution will remain heterogeneous due to poor mixing by diffusion. The re-dissociation of interparticle aggregates may be slower for longer chains, so the high MW fraction will remain the last to become completely solvated.

Furthermore, in our preliminary experiments with turbidimetry and HS-DSC, we have found evidence that PNIPAM made by ATRP (PNIPAM-ATRP) is less colloidally stable than that made by conventional radical polymerization (PNIPAM-AIBN). However, the reason why the PNIPAM-ATRP aggregates are less colloidally stable is still not clear. Plausible reasons include: (a) higher MW chains may act as more efficient steric stabilizer for the aggregates than lower MW PNIPAM; (b) narrow-disperse samples may fold and pack more efficiently and rapidly. In addition, a denser collapsed state with less free volume may be responsible for the slow re-dissolution. Investigation of the effects of MW and polydispersity on the aggregate particle size by dynamic light scattering (DSL) will be the subject of future work.

References

(1) Xia, Y.; Yin, X.; Burke, N. A. D.; Stover, H. D. H. *Macromolecules* **2005**, *38*, 5937-5943.

(2) Fujishige, S.; Kubota, K.; Ando, I. *J. Phys. Chem.* **1989**, *93*, 3311-3313.

(3) Kubota, K.; Fujishige, S.; Ando, I. *J. Phys. Chem.* **1990**, *94*, 5154-5158.

(4) Qiu, X.; Wu, C. *Macromolecules* **1997**, *30*, 7921-7926.

Appendix B. ^{1}H NMR of the Initiators

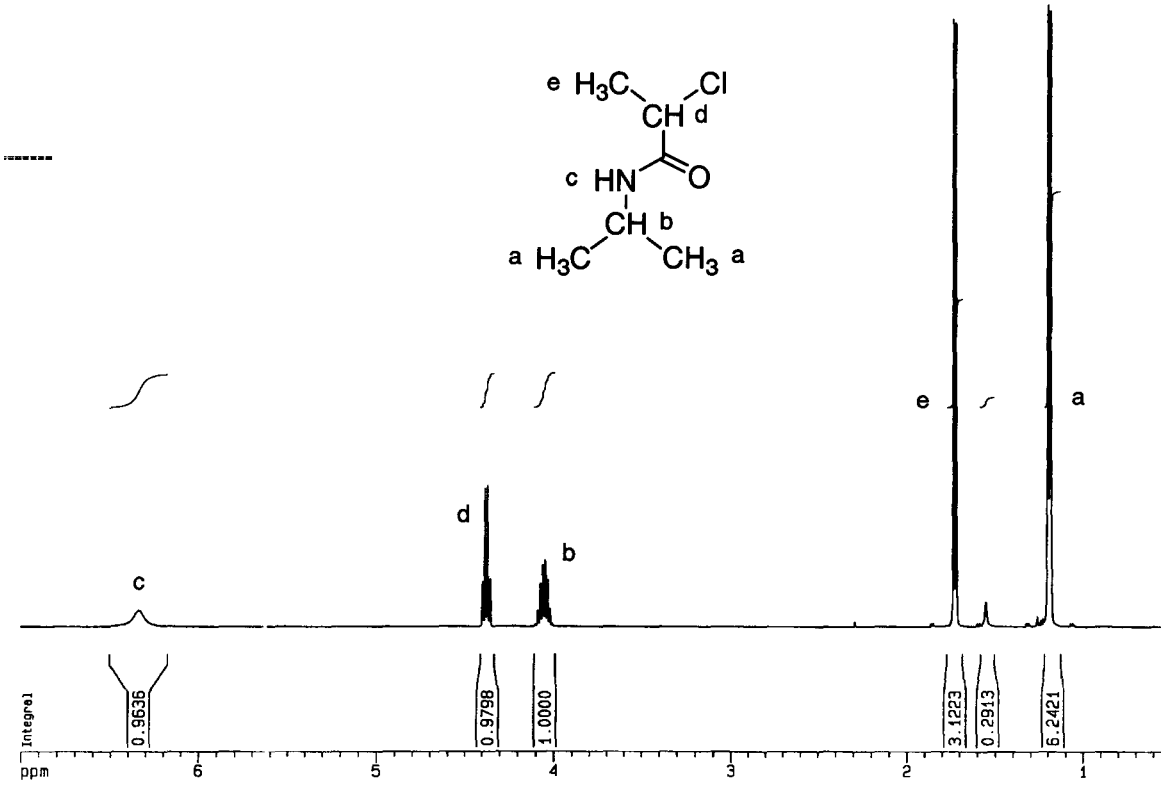

Figure 1. ^{1}H NMR spectrum of *N*-Isopropyl-2-chloropropionamide in $CDCl_3$.

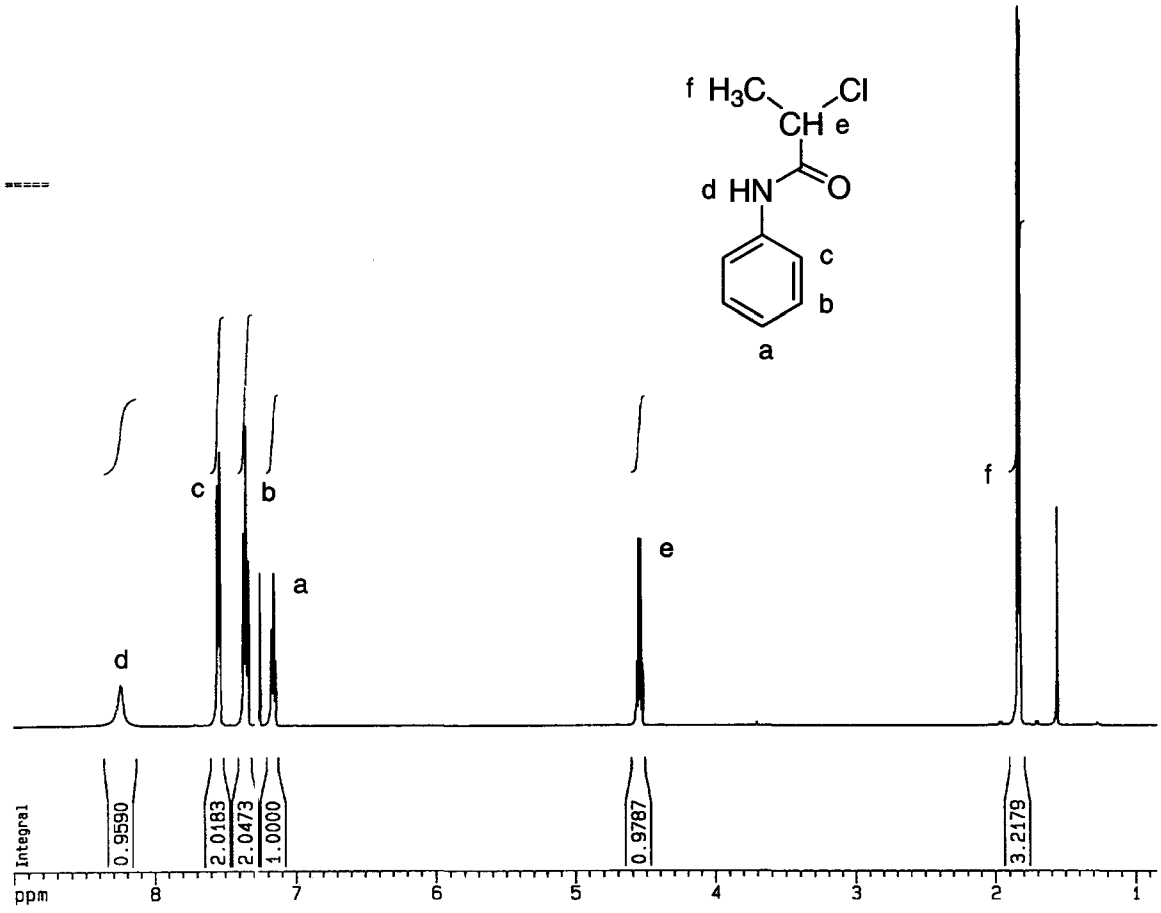

Figure 2. ^{1}H NMR spectrum of *N*-phenyl-2-chloropropionamide in $CDCl_3$.

Appendix C. ^{1}H NMR of PNIPAM

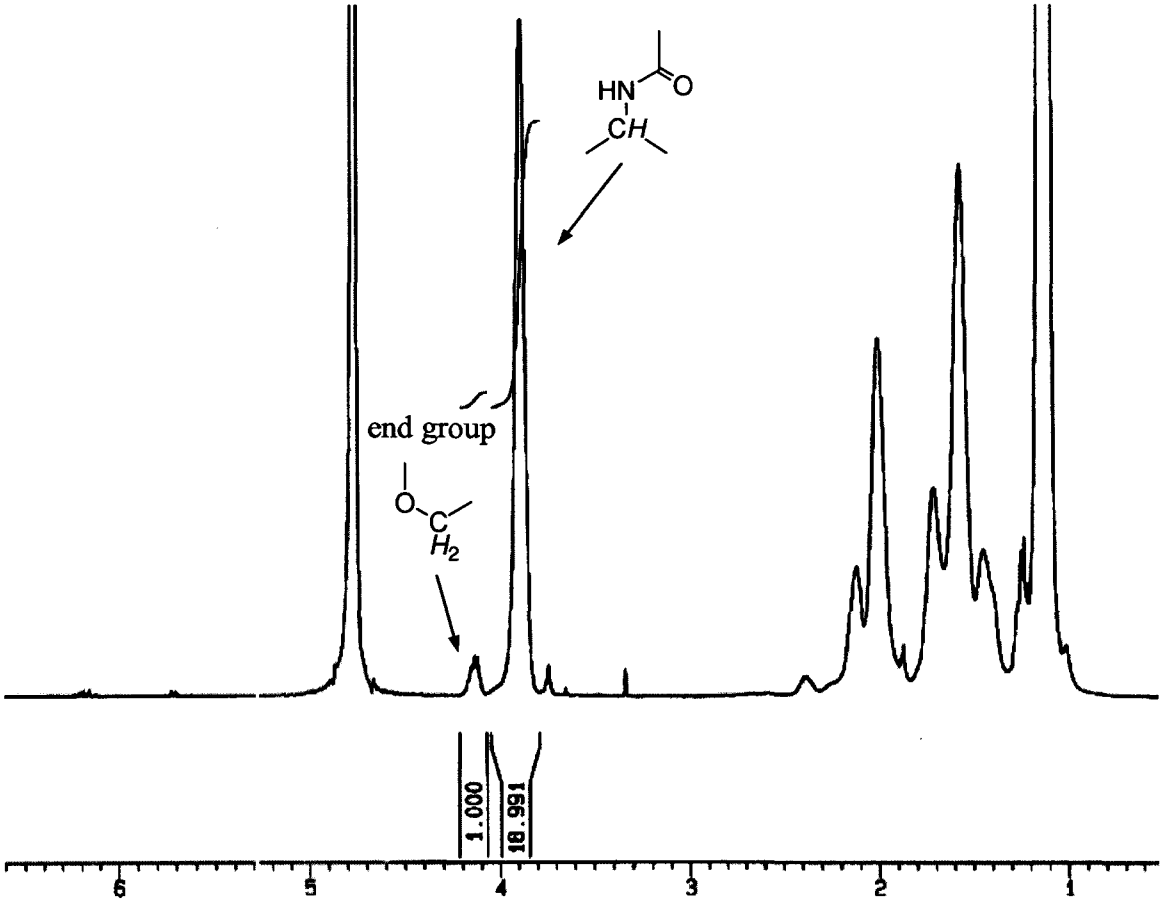

Figure 1. ^{1}H NMR spectrum of PNIPAM-ECP ($M_{n,th}$ = 4.6 kDa) in D_2O.

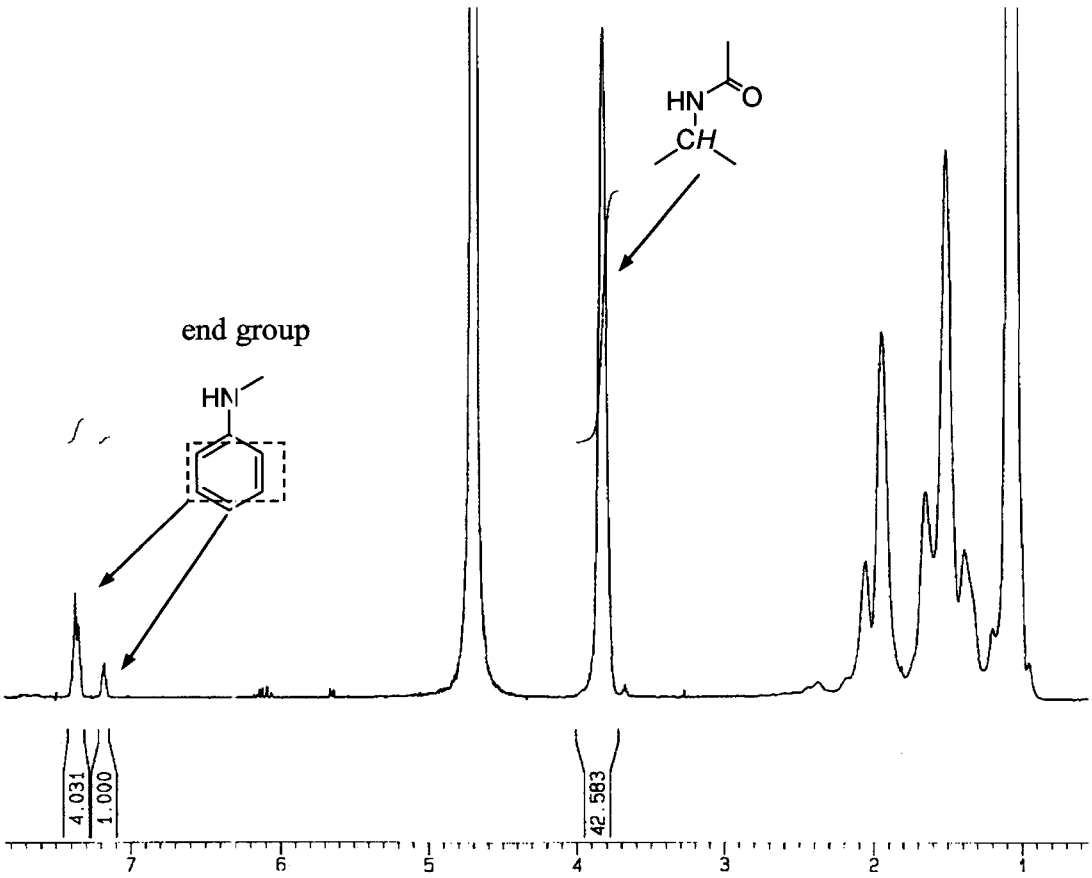

Figure 2. ^{1}H NMR spectrum of PNIPAM-PhCP ($M_{n,th}$ = 4.6 kDa) in D_2O.

Chapter 4 Future Work

4.1 Study of the influence of tacticity on the LCST

It has been reported that the LCST of isotactic poly(diethylacrylamide) (PDEA) is 10 °C higher than syndiotactic PDEA and atactic PDEA.[1] However, broad polydispersity and different end groups may have precluded accurate comparison. Tacticity control in controlled/living radical polymerization has been realized recently using Lewis acids, such as yttrium trifluoromethanesulfonate ($Y(OTf)_3$).[2,3] Employing this approach in the ATRP of NIPAM using *i*-PrCP may give narrow-disperse PNIPAM with well-controlled end group and isotactic structure. Thus, comparison of isotactic and atactic PNIPAM-ATRP may unveil the corporative effect of side groups in isotactic PNIPAM on the LCST without the perturbation from the MW and end group effects. The initial hypothesis would be that an isotactic backbone would facilitate (hydrophobic) chain-chain interactions and hence result in a decreased LCST.

4.2 Application of the ATRP of NIPAM and the MW dependence

The discovered strong MW dependence of the phase transition temperature of PNIPAM may be used to develop multi-step thermoresponsive systems using PNIPAM with different MW for applications in temperature-controlled selective separation or reaction.

The developed ATRP of NIPAM can be extended to graft PNIPAM with well-controlled MW and end groups onto and/or from microspheres and other surfaces. Different grafting chain length may result in selective temperature response. However,

the difference in the thermoresponse between free linear polymer chains and grafted chains has to be studied as the decreased mobility of the tethered chain end may affect the phase transition behavior of the polymer.

Narrow-disperse PNIPAM with different MW and pre-designed functional end groups can also be readily conjugated to different receptor protein, ligand, and catalyst (or enzyme) to give temperature controlled selective protein separation and reactions.

References

(1) Freitag, R.; Baltes, T.; Eggert, M. *J. Polym. Sci. A: Polym. Chem.* **1994**, *32*, 3019-3030.

(2) Lutz, J.-F.; Neugebauer, D.; Matyjaszewski, K. *J. Am. Chem. Soc.* **2003**, *125*, 6986-6993.

(3) Ray, B.; Isobe, Y.; Matsumoto, K.; Habaue, S.; Okamoto, Y.; Kamigaito, M.; Sawamoto, M. *Macromolecules* **2004**, *37*, 2268-2274.